Cureus Journal of Engineering

Open Access Original Article

Characteristics of a Rotating Rivlin-Ericksen Fluid Model: Impact of Radiation Absorption, Hall and Ion Slip Currents on Magnetohydrodynamic Free Convective Flow over a Vertical Porous Plate

Received 10/16/2024
Review began 10/17/2024
Review ended 05/20/2025
Published 07/21/2025

DOI: https://doi.org/10.7759/s44388-024-01410-9

KVB Rajakumar [1] , T Govinda Rao [2] , TRKD Vara Prasad [3] , G Sreenivasulu [4]

1. Department of Mathematics, Kallam Haranadhareddy Institute of Technology, Guntur, IND 2. Department of Mathematics, Seshadri Rao Gudlavalleru Engineering College, Gudlavalleru, IND 3. Department of Mathematics, SRKR Engineering College, Bhimavaram, IND 4. Department of Physics, Kallam Haranadhareddy Institute of Technology, Guntur, IND

Corresponding author: KVB Rajakumar, kvbrajakumar@gmail.com

Abstract

The current study examines the characteristics of a rotating Rivlin-Ericksen fluid model influenced by radiation absorption, Hall and ion slip current on magnetohydrodynamic free convective flow over an impulsively started infinite vertical porous plate, considering the Dufour and chemical reaction effects. The Rivlin-Ericksen model provides a mathematical framework for describing non-Newtonian fluids, which exhibit complex behaviors such as shear-thinning, shear-thickening, viscoelasticity, and nonlinearity, deviating from the simple stress-strain relationship observed in Newtonian fluids. Analytical solutions to the governing partial differential equations are obtained, examining the axial and transverse velocity components, temperature, and concentration profiles across various physical parameters. Additionally, skin friction, Nusselt number, and Sherwood number are analyzed and presented in tabular form. The results demonstrate that increasing angular rotation, magnetic field strength, chemical reaction, and radiation parameters reduce both primary and secondary velocity components. Conversely, radiation absorption and heat source parameters have the opposite effect. The study also highlights significant variations in skin friction, Nusselt number and Sherwood number, influenced by factors such as Hall and ion slip currents, Schmidt number, Prandtl number, Dufour effect, and thermal radiation. The results offer practical insights for optimizing thermal and fluid control in aerospace, nuclear, and petroleum applications.

Categories: Thermal and Fluid Systems
Keywords: rivlin-ericksen fluid, magnetohydrodynamics, dufour effect, hall and ion-slip current, porous plate, chemical reaction, radiation absorption

Introduction

The study of non-Newtonian fluids has garnered considerable attention due to their complex dynamics under various flow conditions. One such class of fluids is the Rivlin-Ericksen fluid, which exhibits characteristics that are distinct from those of classical Newtonian fluids, such as shear-dependent viscosity and normal stress differences. The Rivlin-Ericksen fluid model is widely employed to describe such dynamics, providing a robust framework for understanding fluid mechanics in complex systems. In this research, the focus is on the rotating Rivlin-Ericksen fluid model, which introduces rotational effects into the fluid's properties. Rotation can significantly impact the stability and flow patterns of such fluids, making it a critical factor in various engineering and geophysical applications, such as rotating machinery, oceanography, and atmospheric flows. The objective of this research is to explore the dynamic response, stability criteria, and flow structures of a Rivlin-Ericksen fluid under the influence of rotational forces. Previous studies have investigated similar themes in the context of Rivlin-Ericksen fluids and their variations. These studies are interconnected through their exploration of complex fluid dynamics, particularly in the context of non-Newtonian fluids, magnetohydrodynamics (MHD), and viscoelastic properties. The influence of Hall effects on unsteady MHD flow in Rivlin-Ericksen fluids, as examined by [1], serves as a foundation for understanding how magnetic fields interact with fluid flow. Building on this, [2] expanded the analysis to third-grade Rivlin-Ericksen fluids, investigating unsteady hydromagnetic behavior in Stokes' second problem, further linking magnetic and fluid dynamics. In [3], the focus shifts to viscoelastic fluid flow on a permeable shrinking sheet, considering additional factors like heat transfer and thermal radiation, which are critical for practical applications involving varying surface temperatures. Similarly, [4] proposed a model that extended these ideas by accounting for the impact of variable fluid properties and a stretchable plate, introducing new complexities to the understanding of viscoelastic fluid deeds. The work in [5] builds upon these ideas by studying hydromagnetic viscoelastic fluid flow over a stretching surface, with particular attention to nonuniform heat sources and sinks, thereby adding another dimension to the fluid-heat interaction. Meanwhile, [6] focused on the influence of Hall currents on unsteady second-grade fluid flow in rotating systems, bridging the gap between MHD performance and rotational effects. Together, these studies lay the groundwork for further research, such as the present work, which delves into the interaction between rotational effects and non-Newtonian fluid characteristics in Rivlin-Ericksen fluids, combining insights from MHD, viscoelasticity, heat transfer, and rotational dynamics.

In the presence of electromagnetic fields, the dynamics of fluids become increasingly complex, leading to the field of MHD. MHD integrates the principles of fluid mechanics and electromagnetism to describe the flow of electrically conducting fluids under the influence of magnetic fields. These flows are vital in various engineering and geophysical applications, such as plasma dynamics, astrophysics, nuclear reactor cooling systems, and MHD power generation. By incorporating the Rivlin-Ericksen fluid model into the MHD framework, we can gain a deeper understanding of the response of non-Newtonian conducting fluids subjected to electromagnetic forces. This research explores the combined effects of the Rivlin-Ericksen fluid model and MHD. In particular, it seeks to examine how magnetic fields affect the flow characteristics, stability, and stress distribution of Rivlin-Ericksen fluids under different boundary conditions. Previous studies offer a strong foundation in this area. Researchers such as [7] investigated the chemical reactions in unsteady MHD convective flow of a second-grade fluid over an unbounded vertical absorbent plate. Unsteady MHD flow of a second-grade fluid through a porous medium, accounting for radiation absorption, diffusion-thermo, as well as Hall and ion slip effects, was studied by [8]. The effects of MHD and radiation on the axisymmetric flow of non-Newtonian fluids over a porous shrinking or stretching surface were studied [9]. Heat and mass transfer in an MHD boundary layer flow of second-grade nanofluids over an inclined stretching permeable surface within a porous medium was studied [10]. The influence of magnetic fields on fluid flow and heat transfer was reviewed, highlighting current advancements and potential future research directions [11]. Furthermore, the combined effects of MHD and mass transpiration on Rivlin-Ericksen fluid flow over a stretching sheet in a porous medium, with a focus on thermal interaction, were investigated [12].

The introduction of Hall and ion slip effects into the study of a Rivlin-Ericksen fluid under the influence of a magnetic field substantially increased the complexity of the system. The Hall effect, which refers to the generation of an electric field perpendicular to both the magnetic field and current in a conducting fluid, becomes particularly relevant in high-conductivity fluids. The magnetic field's interaction with the fluid leads to nonlinear effects on the flow [13]. The ion slip effect, on the other hand, represents the relative motion between electrons and ions under a magnetic field, causing an additional deviation in the current density. Both the Hall and ion slip effects modify the electromagnetic forces acting on the fluid, altering its velocity, temperature distribution, and boundary layer characteristics. By incorporating these effects into the Rivlin-Ericksen fluid model, researchers sought to explore how electromagnetic phenomena influence non-Newtonian fluid deeds. This research has implications for understanding heat and mass transfer, material processing, and natural phenomena. This study investigates the influence of Hall and ion slip currents on the flow and heat transfer characteristics of Rivlin-Ericksen fluids in various geometric configurations. By analyzing the impact of these parameters on velocity profiles, temperature fields, and energy dissipation, the research provides valuable insights into the interaction between electromagnetic fields and non-Newtonian fluid mechanics. In previous studies, unsteady MHD flow of Walter's liquid model-B was examined, incorporating effects such as Dufour, thermal radiation, chemical reactions, Hall and ion slip currents [14]. Further research analyzed the influence of Hall and ion slip currents on the rheological properties of viscoelastic fluids [15]. Viscous dissipation in convective chemically reacting Rivlin-Ericksen fluid flow around a porous vertical plate was also investigated, but Hall and ion slip currents were excluded in this case [16]. Additionally, insights were provided into thermal convection performance in dusty compressible Rivlin-Ericksen viscoelastic fluids, accounting for Hall currents [17]. The effect of Hall currents on rotating oscillating flows of Oldroyd-B fluid in porous media was studied [18], while nonlinear heat and mass transfer in second-grade fluid flow, considering Hall currents and thermophoresis, was explored [19]. Lastly, heat and mass transfer in three-dimensional radiative MHD Casson fluid flow over a stretching permeable sheet, with a chemical reaction, was analyzed [20]. These studies contribute to understanding the interplay between fluid dynamics and electromagnetic phenomena, offering valuable insights for practical applications.

Chemical reactions significantly impact the properties of viscoelastic fluids. They can alter viscosity, influence flow dynamics, and modify microstructural characteristics. Factors like reaction kinetics, temperature dependency, and product formation play crucial roles in these changes. Understanding these influences is essential for tailoring viscoelastic fluids to specific applications. Researchers have explored diverse aspects of unsteady MHD flows of second-grade fluids through porous media, considering various physical phenomena such as radiation absorption, chemical reactions, and aligned magnetic fields. The influence of Hall and rotational effects on unsteady MHD rotating flows was examined [21]. The impacts of radiation absorption and ion slip effects in such flows were also studied [22], while the role of Hall effects on heat and mass transfer was further explored [23]. Research into the effects of radiation, heat generation/absorption, and chemical reactions in MHD flows was conducted [24]. Additionally, the impact of chemical reactions on MHD convective flows through absorbent media, considering ramped wall temperature and surface concentration, was investigated [25]. This research contributes to a deeper understanding of the complex interactions between chemical reactions, fluid rheology, and external physical forces, facilitating advancements in various technological domains.

The Dufour effect, which describes the coupling between temperature gradients and mass diffusion, becomes particularly relevant when applied to Rivlin-Ericksen fluid models in MHD flows. The Rivlin-Ericksen model provides a framework for understanding the actions of complex non-Newtonian fluids under stress. By incorporating the Dufour effect, we can investigate how temperature variations influence both the stress within the fluid and the diffusion of its components. This interplay between the Dufour effect and Rivlin-Ericksen fluid models has significant implications for heat transfer and fluid dynamics in various engineering applications. A thorough understanding of these interactions is essential for optimizing processes involving complex fluids in MHD systems. Several studies have explored the influence of Dufour effects on various fluid dynamics scenarios. Mixed convection in a chemically reacting couple stress fluid within a vertical channel was investigated [26]. Free convective flow over a vertical plate, considering Dufour effects in a doubly stratified medium, was studied [27]. The influence of MHD forces on double-diffusive convection along a wavy surface in a porous medium, under the combined Soret and Dufour effects, was analyzed [28]. Dufour effects in MHD heat and mass transfer of viscoelastic fluid over a semi-infinite plate was examined [29]. Chemically reactive MHD flow within a wavy channel was also explored [30], while mixed convection of Casson and Oldroyd-B fluids over a stratified stretching sheet, incorporating nonlinear thermal radiation and chemical reaction was studied [31].

Previous investigations of unsteady magnetohydrodynamic free convective flow past an impulsively started infinite vertical porous plate have often neglected the influence of the rotating Rivlin-Ericksen fluid model along with radiation absorption, chemical reaction, as well as the Dufour effect. This study expands upon the work of [14] by incorporating these factors and exploring their impact on the flow performance. The perturbation method is used to evaluate the governing equations, and the results for velocity, temperature, and concentration are presented graphically. Skin friction, Nusselt number, and Sherwood number are tabulated. The findings of this study align well with previous research. The findings of this study are applicable to engineering systems involving non-Newtonian fluid behavior under magnetic fields and rotational effects, such as in aerospace cooling systems, nuclear reactor thermal regulation, and petroleum extraction processes. The inclusion of Hall and ion-slip currents, chemical reactions, and radiation absorption provides valuable insights for the design and optimization of heat exchangers, magneto-fluidic devices, and industrial processes involving electrically conducting and reactive fluids.

Materials And Methods

The Rivlin-Ericksen fluid model is characterized by a set of constitutive equations that describe the stress-strain relationship for viscoelastic fluids. These equations account for the time-dependent deeds of the fluid and incorporate both the rate of deformation and the history of deformation. Below are the key equations associated with the Rivlin-Ericksen fluid model:

$$[p_{ik} = -\rho g_{ik} + p^*_{ik}] \quad (1)$$

$$[p^*_{ik} = 2\int_{-\infty}^{t} \xi\,(t-t^*) e^{(1)}_{ik}(t^*)dt^*] \quad (2)$$

Where $\xi(t-t^*) = \int_0^{\infty} \frac{N(\tau)}{\tau} \exp\left(-\left(\frac{t-t^*}{\tau}\right)\right) d\tau$ (3)

p_{ik}: stress, tensor

p: arbitrary isotropic pressure

$g_{ik};$: metric tensor of a fixed coordinate system

$[x^i e^{(1)}_{ik}]$: rate of strain tensor

$N(\tau)$: distribution function of relaxation time

Equation (2) can be put in the following generalized form which is valid for all types of motion and stress:

$$[p^*_{ik} = 2\int_{-\infty}^{t} \xi\,(t-t^*)\ \frac{\partial x^i}{\partial x^*_m}.\frac{\partial x^k}{\partial x^*_r}\ e^{(1)}_{mr}\ \ (x^*\,t^*)\,dt^*] \quad (4)$$

$x^{*\,i}$: position at the time t^* of the element that is instantaneously at the print x^i at time‘t’.

The fluid with equation of state (1) and (4) has been designated as liquid B^*.

In the case of liquids with short memories, that is short relaxation time, the above equation of state can be written in the flowing simplified form.

$$p_{ik}^{*}\left(x,t\right)=2\eta_{0}e_{ik}^{(1)}-2k_{0}\frac{\partial e_{ik}^{(1)}}{\partial t} \quad (5)$$

$\eta_0=\int_0^{\infty}N(\tau)\mathrm{d}\tau$: limiting viscosity at small rates of shear

$k_0=\int_0^{\infty}\tau N(\tau)\ \mathrm{d}\tau$: visco-elasticity parameter

\frac{\partial }{{\partial t}}\: convicted time derivative.

This adaptable and resilient rheological model has a simple mathematical formulation that may be easily integrated into boundary layer theory for practical applications.

The characteristics of mathematical model.

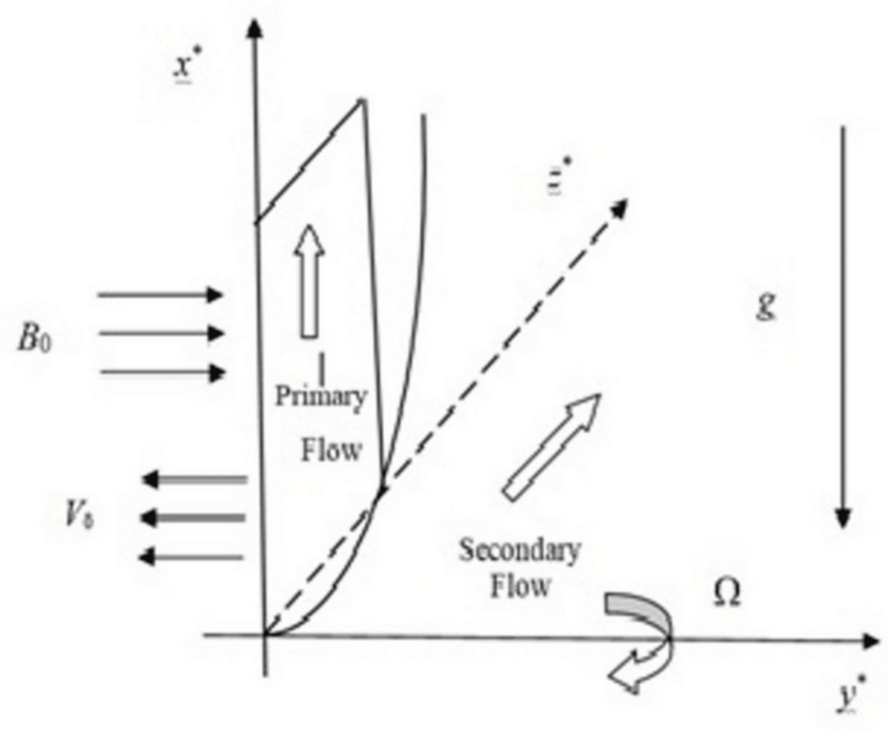

FIGURE 1: Physical model of the problem

The mathematical formulation of the problem involves analyzing the unsteady flow of a viscous, incompressible, and electrically conducting fluid under the following conditions:

Fluid Dynamics: The fluid flow past an infinite vertical porous plate, as depicted in Figure 1.

Porous Medium: The plate is embedded in a porous medium and experiences fluctuating temperature and concentration.

Magnetic Field: A uniform magnetic field B_0 is applied perpendicular to the flow.

Coordinate System: The coordinate system (x*, y*, z*) is defined such that the x*-axis runs along the plate's surface in the upward-right direction, the y*-axis is perpendicular to the plate's surface while z*-axis is considered along the width of the plate as shown in Figure 1.

Velocity of the Plate: The plate starts moving with an initial velocity U_0 within its plane.

Vacuum Velocity: An initial suction or vacuum velocity V_0 is imparted to the porous plate.

Dependence on Coordinates: Due to the infinite length of the plate, all physical variables depend only on the y* - coordinate and time t*.

Negligible Magnetic Induction: The induced magnetic field is negligible due to the low magnetic Reynolds number, allowing the magnetic field effects to be simplified.

Electron Pressure: Electron pressure is assumed constant, and the electric field vector is zero in the absence of an externally applied electric field.

Negligible Energy Dissipation: Due to the intrinsic resistance of the fluid molecules, energy dissipation is minimal.

Thermodynamic Considerations: The energy equation incorporates heat sources, thermal radiation, and the Dufour effect (energy transport due to mass diffusion).

Angular Momentum: The angular momentum is factored into the momentum equation to account for rotational effects.

Chemical Reactions: The rate constant Kr accounts for homogeneous chemical reactions among species dispersing in the fluid.

By assuming B_0 has been taken into account wherever in the fluid (B_0 is a constant) using the magnetic field B = (B_x, B_y, B_z) relation. The relation J = 0 yields J_y = constant if the current density is represented by J = (J_x, J_y, J_z). As a result the plate is not carrying electricity, J_y = 0 at the surface and, by furtherance, 0 anywhere else.

The transformed form of Ohm's law regarding current in a generic magnetic field is as outlined below:

$$\overline{J} = \sigma\left(1 + \left(\xi\left(J_{\mathrm{e}}\right)^{-1}\right)^{2}\right)^{-1}\left(\overline{E} + (\overline{V}\times\overline{B}) - \left(\mathrm{en}_{\mathrm{e}}\right)^{-1}\left(\overline{J}\times\overline{B}\right)\right) \quad (6)$$

ω: is the electron cyclotron

$[\vartheta_e]$: electron-atom collision frequency.

When the ratio $\left[\omega(\vartheta_e)^{-1}\right]$ is very large, the phenomenon is called Ion-slip.

This formulation sets up a system of partial differential equations governing the fluid velocity, temperature, and concentration subject to the given boundary conditions and physical assumptions.

Continuity equation

$$\frac{\partial v^*}{\partial y^*} = 0 \ \Rightarrow v^* = -V_0 \quad (7)$$

Momentum equation

$$(frac\partial u^*\partial t^* + v^*\frac{\partial u^*}{\partial y^*} = \frac{\eta_0}{\rho}\frac{\partial^2 u^*}{\partial y^{*2}} + 2\Omega w^* - \frac{k_0}{\rho}\left(\frac{\partial^3 u^*}{\partial t^*\partial y^{*2}} + v^*\frac{\partial^3 u^*}{\partial y^{*2}}\right) + g\beta\left(T^* - T^*_\infty\right) - \frac{\upsilon u^*}{K^*}, + g\beta^*\left(C^* - C^*_\infty\right) - \frac{\sigma B_0^2\left[\left(1+\beta_e\beta_i\right)u^* + \beta_e w^*\right]}{\rho\left[\left(1+\beta_e\beta_i\right)^2 + \beta_e^2\right]} \quad (8)$$

$$(\frac{\partial w^*}{\partial t^*} + v^*\frac{\partial w^*}{\partial y^*} = \frac{\eta_0}{\rho}\frac{\partial^2 w^*}{\partial y^{*2}} - 2\Omega u^* - \frac{k_0}{\rho}\left(\frac{\partial^3 w^*}{\partial t^*\partial y^{*2}} + v^*\frac{\partial^3 w^*}{\partial y^{*2}}\right) - \frac{\upsilon w^*}{K^*} - \frac{\sigma B_0^2\left[\left(1+\beta_e\beta_i\right)w^* + \beta_e u^*\right]}{\rho\left[\left(1+\beta_e\beta_i\right)^2 + \beta_e^2\right]} \quad (9)$$

Energy equation

$$\frac{\partial T^*}{\partial t^*} + v^*\frac{\partial T^*}{\partial y^*} = \frac{k_T}{\rho C_p}\frac{\partial^2 T^*}{\partial y^{*2}} - \frac{1}{\rho C_P}\frac{\partial q_r^*}{\partial y^*} + Q_0\left(T^* - T^*_\infty\right) + \frac{DK_T}{C_p C_s}\frac{\partial^2 C^*}{\partial y^{*2}} + R^*\left(C^* - C^*_\infty\right)$$

(10)

Concentration equation

$$\frac{\partial C^*}{\partial t^*}+v^*\frac{\partial C^*}{\partial y^*}=D\frac{\partial^2 C^*}{\partial {y^*}^2}-K_1\left(C^*-C^*_\infty\right) \quad (11)$$

Depending on the parameters of the boundaries

$$\left[\begin{array}{l} u^*=U_0,\ w^*=0,\ \theta^*=a\,e^{i\omega^* t^*},\ \phi^*=be^{i\omega^* t^*}\ as\ \ y^*=0 \\ u^*\to 0,\ w^*\to 0,\ \theta^*\to 0,\ \phi^*\to 0 \qquad\qquad at\, y^*=\infty \end{array}\right\} \quad (12)$$

Bring up the amounts that are not based on dimensions,

$$y=\frac{V_0}{\upsilon}y^*,\ t=\frac{V_0^2 t^*}{4\upsilon},\ u=\frac{u^*}{V_0},\ w=\frac{w^*}{V_0},\ T^*-T^*_\infty=\theta^*,\ C^*-C^*_\infty=\psi^*,\theta=\frac{\theta^*}{a},\ \psi=\frac{\psi^*}{b}$$

(13)

The radiative heat flux term by using the Rosseland approximation is given by

$$q_r^*=-\frac{4\sigma_s^*}{3k_e^*}\frac{\partial {T^*}^4}{\partial y^*} \quad (14)$$

It was assumed that the temperature difference within the flow is sufficiently small such that ${T^*}^4$ can be expressed as a linear function of the temperature; this is expanding in Taylor series about T^*_∞ and neglecting higher order terms to give:

$$T^*\cong 4T^*{T^*_\infty}^3-3T^*_\infty \quad (15)$$

Substitute Equations (13)-(15) in the Equations (8)-(11) then we get following governing equations which are dimensionless:

$$\left[\frac{1}{4}\frac{\partial u}{\partial t}-\frac{\partial u}{\partial y}=\frac{\partial^2 u}{\partial y^2}+2\,S\,w-k\left(\frac{1}{4}\frac{\partial^3 u}{\partial t\partial y^2}-\frac{\partial^3 u}{\partial y^3}\right)-\left(\frac{M\alpha_e u+\beta_e\,w}{{\alpha_e}^2+\ \beta_e^2}\right)+Gr\theta+Gm\phi-\frac{u}{K}\right]$$

(16)

$$\frac{1}{4}\frac{\partial w}{\partial t}-\frac{\partial w}{\partial y}=\frac{\partial^2 w}{\partial y^2}-2\,S\,u-k\left(\frac{1}{4}\frac{\partial^3 w}{\partial t\partial y^2}-\frac{\partial^3 w}{\partial y^3}\right)-\left(\frac{M\alpha_e w-\beta_e u}{{\alpha_e}^2+\beta_e^2}\right)-\frac{w}{K}$$

(17)

$$\frac{1}{4}\frac{\partial \theta}{\partial t}-\frac{\partial \theta}{\partial y}=\frac{1}{Pr}\left(1+\frac{4}{3R}\right)\frac{\partial^2\theta}{\partial y^2}+Dr\frac{\partial^2\psi}{\partial y^2}+F\theta+Ra\ \psi \quad (18)$$

$$\left[\frac{1}{4}\frac{\partial \psi}{\partial t}-\frac{\partial \psi}{\partial y}=\frac{1}{Sc}\frac{\partial^2\psi}{\partial y^2}-\gamma\ \psi\right] \quad (19)$$

The relevant boundary conditions are as follows:

$$\left[\left.\begin{array}{l} u=1,\ w=0,\ \theta=e^{i\,\omega\,t},\ \psi=e^{i\,\omega\,t}\quad as\ \ y=0 \\ u\to 0,\ w\to 0,\ \theta\to 0,\ \psi\to 0\quad at\ \ y=\infty \end{array}\right\}\right] \quad (20)$$

Introducing the complex variable $F=u\left(y,t\right)+iw\left(y,t\right)](21)$

Where $[i=\sqrt{-1}$

Combine Equation (16) and Equation (17) by using the relation (21) then we obtained transformed single partial differential equation.

$$\frac{1}{4}\frac{\partial F}{\partial t}-\frac{\partial F}{\partial y}=\frac{\partial^2 F}{\partial y^2}-k\left(\frac{1}{4}\frac{\partial^3 F}{\partial t\partial y^2}-\frac{\partial^3 F}{\partial y^3}\right)-NF+Gr\theta+Gm\ \psi \quad (22)$$

Corresponding boundary conditions are as follows:

$$\left.\begin{array}{l} y=0: \quad F=1, \quad \theta=e^{i\,\omega\,t}, \;\; \psi=e^{i\,\omega\,t} \\ y=\infty: \quad F\rightarrow 0, \; \theta\rightarrow 0, \;\; \psi\rightarrow 0 \end{array}\right\} \text{(23)}$$

Here

$$\begin{array}{l} Gr=\frac{g\beta(T^{*}-T^{*}_{\infty})a}{V_0^3}, Gm=\frac{g\beta^{*}(C^{*}-C^{*}_{\infty})b}{V_0^3}, M=\frac{\sigma\upsilon B_0^2}{\rho V_0^2}, K=\frac{K^{*}V_0^2}{\upsilon^2}, R=\frac{4\sigma^{*}T^{3}_{\infty}}{kk^{*}} \\ \left[\;\gamma=\frac{\upsilon K_1}{V_0^2}, k=\frac{k_0V_0^2}{\rho\upsilon^2}, Dr=\frac{bDK_T}{a\upsilon C_p}, Ra=\frac{bR^{*}\upsilon}{aV_0^2}, F=\frac{Q\upsilon}{V_0^2}, Sc=\frac{\upsilon}{D}, \Gamma=\frac{1}{\mathrm{Pr}}\left(1+\frac{4}{3R}\right)\right. \end{array}$$

(24)

In order to solve Equations (18), (19), and (22) under the boundary conditions of (23) we use single perturbation method, so assume that

$$\left.\begin{array}{l} F\left(y,t\right)=F_0\left(y\right)\;e^{i\omega t} \\ \theta\left(y,t\right)=\theta_0\left(y\right)\;e^{i\omega t} \\ \psi\left(y,t\right)=\psi_0\left(y\right)\;e^{i\omega t} \end{array}\right\} \text{(25)}$$

Substituting (25) in the Equations (18), (19), and (22) then we obtained the following differential equations:

$$kF_0^{'''}+\left(1-\frac{ik\omega}{4}\right)F_0^{''}+F_0^{'}-NF_0=-\mathrm{Gr}\theta_0-\mathrm{Gm}\phi_0 \text{ (26)}$$

$$\mathit{\Gamma}\theta_0^{''}+\theta_0^{'}-\left(-F+\frac{i\omega}{4}\right)\theta_0=-\mathrm{Dr}\phi_0^{''}-\mathrm{Ra}\phi_0 \text{ (27)}$$

$$\psi_0^{''}+\mathrm{Sc}\psi_0^{'}-\mathrm{Sc}\left(\gamma+\frac{i\omega}{4}\right)\psi_0=0 \text{ (28)}$$

The corresponding transformed boundary conditions are as follows:

$$\left.\begin{array}{l} y=0: \quad F_0=e^{-i\,\omega\,t}, \;\; \theta_0=1, \;\; \psi_0=1 \\ y=\infty: \quad F_0\rightarrow 0, \;\; \theta_0\rightarrow 0, \;\; \psi_0\rightarrow 0 \end{array}\right\} \text{(29)}$$

To solve Equation (26), we use the multi parameter perturbation technique as follows:

$$F_0=F_{00}(y)+k_1F_{01}(y) \text{ (30)}$$

as k1<<1, for smallest quantity.

Using (30) in the Equation (26) and equating the coefficient of like powers of k1, and then we get:

$$F_{00}^{''}+F_{00}^{'}-NF_{00}=-\mathrm{Gr}\theta_0-\mathrm{Gm}\Psi_0 \text{ (31)}$$

$$F_{01}^{''}+F_{01}^{'}-NF_{01}=\frac{i\omega}{4}F_{00}^{''}-F_{00}^{'''} \text{ (32)}$$

$$\left.\begin{array}{l} y=0: \quad F_{00}=\mathrm{e}^{-i\,\omega\,t}, \; F_{01}=0, \;\; \theta_0=1, \;\; \psi_0=1 \\ y=\infty: \quad F_{00}\rightarrow 0, \;\; F_{01}\rightarrow 0, \quad \theta_0\rightarrow 0, \; \psi_0\rightarrow 0 \end{array}\right\} \text{(33)}$$

Solve Equations (27), (28), (31), and (32) by utilizing (35) then we obtain

$$F_0=\left(A_1e^{-m_3y}+h_3e^{-m_1y}+k_1h_5e^{-m_2y}\right)+i\;\;\left(h_2e^{-m_2y}+k_1h_4e^{-m_1y}+k_1\left(h_6+A_2\right)e^{-m_3y}\right)$$

(34)

$$\theta_0=A_0e^{-m_2y}+h_1e^{-m_1y} \text{ (35)}$$

$$\psi_0=e^{-m_1y} \text{ (36)}$$

Substitute the Equations (34)-(36) in the (25) then we obtain:

$$[F(y,t) = \left[\left(A_1 e^{-m_3 y} + h_3 e^{-m_1 y} + k_1 h_5 e^{-m_2 y}\right) + i\left(h_2 e^{-m_2 y} + k_1 h_4 e^{-m_1 y} + k_1 (h_6 + A_2) e^{-m_3 y}\right)\right] e^{i\omega t}]$$
(37)

Now, equating the real and imaginary part, it was obtained the axial as well as transverse components of velocity as follows:

$$[\left.\begin{array}{c} u = (A_1 e^{-m_3 y} + h_3 e^{-m_1 y} + k_1 h_5 e^{-m_2 y})\, Cos\omega t \\ -(h_2 e^{-m_2 y} + k_1 h_4 e^{-m_1 y} + k_1 (h_6 + A_2) e^{-m_3 y})\ sin\omega t \end{array}\right\}] \quad (38)$$

$$[\left.\begin{array}{c} w = (h_2 e^{-m_2 y} + k_1 h_4 e^{-m_1 y} + k_1 (h_6 + A_2) e^{-m_3 y})\, Cos\omega t \\ +(A_1 e^{-m_3 y} + h_3 e^{-m_1 y} + k_1 h_5 e^{-m_2 y})\, Sin\omega t \end{array}\right\}] \quad (39)$$

$$\theta(y,t) = A_0 e^{(i\omega t - m_2 y)} + N_1 e^{(i\omega t - m_1 y)} \quad (40)$$

$$\psi(y,t) = e^{(i\omega t + m_1 y)} \quad (41)$$

Skin Friction:

The axial component of the shearing stress at the plate for primary velocity is

$$\chi_1 = \left[\frac{\partial u}{\partial y} - k_1\left(\frac{1}{4}\frac{\partial^2 u}{\partial t \partial y} - \frac{\partial^2 u}{\partial y^2}\right)\right]_{y=0} \quad (42)$$

$$\chi_1 = \left(\begin{array}{c} [(-m_3 A_1 - m_1 h_3 - m_2 k_1 h_5)\,\mathrm{Cos}\omega t - (-m_2 h_2 - m_1 k_1 h_4 - m_3 k_1 (h_6 + A_2))\,\sin\omega t]\ - \\ k_1 \left(\begin{array}{c} \frac{\omega}{4}[(m_3 A_1 + m_1 h_3 + m_2 k_1 h_5)\,\mathrm{Sin}\omega t - (-m_2 h_2 - m_1 k_1 h_4 - m_3 k_1 (h_6 + A_2))\ Cos\omega t] \\ -[(-m_3^2 A_1 - m_1 h_3 - m_2^2 k_1 h_5)\,\mathrm{Cos}\omega t - (-m_2^2 h_2 - m_1^2 k_1 h_4 - m_3^2 k_1 (h_6 + A_2))\,\sin\omega t] \end{array}\right) \end{array}\right)$$
(43)

The transverse component of the shearing stress at the plate for secondary velocity is

$$\chi_2 = \left[\frac{\partial w}{\partial y} - k_1\left(\frac{1}{4}\frac{\partial^2 w}{\partial t \partial y} - \frac{\partial^2 w}{\partial y^2}\right)\right]_{y=0} \quad (44)$$

$$\chi_2 = \left(\begin{array}{c} [(-m_2 h_2 - m_1 k_1 h_4 - m_3 k (h_6 + A_2))\ Cos\omega t - (m_3 A_1 + m_1 h_3 + m_2 k h_5)\, Sin\omega t]\ - \\ k_1 \left(\begin{array}{c} \frac{\omega}{4}[(m_2 h_2 + m_1 k_1 h_4 + m_3 k (h_6 + A_2))\ Sin\omega t - (m_3 A_1 + m_1 h_3 + m_2 k_1 h_5)\, Cos\omega t] \\ -[(m_2^2 h_2 + m_1^2 k_1 h_4 + m_3^2 k (h_6 + A_2))\ Cos\omega t + (m_3^2 A_1 + m_1^2 h_3 + m_2^2 k_1 h_5)\, Sin\omega t] \end{array}\right) \end{array}\right)$$
(45)

Nusselt number:

The rate of heat transfer in terms of the Nusselt number is given by

$$N_w = \left(\frac{\partial \theta}{\partial y}\right)_{y=0} = m_2 A_0 e^{i\omega t} + m_1 h_1 e^{i\omega t} \quad (46)$$

Sherwood number:

The rate of mass transfer coefficient in terms of the Sherwood number is given by

$$S_h = \left(\frac{\partial \psi}{\partial y}\right)_{y=0} = m_1 e^{i\omega t} \quad (47)$$

Results

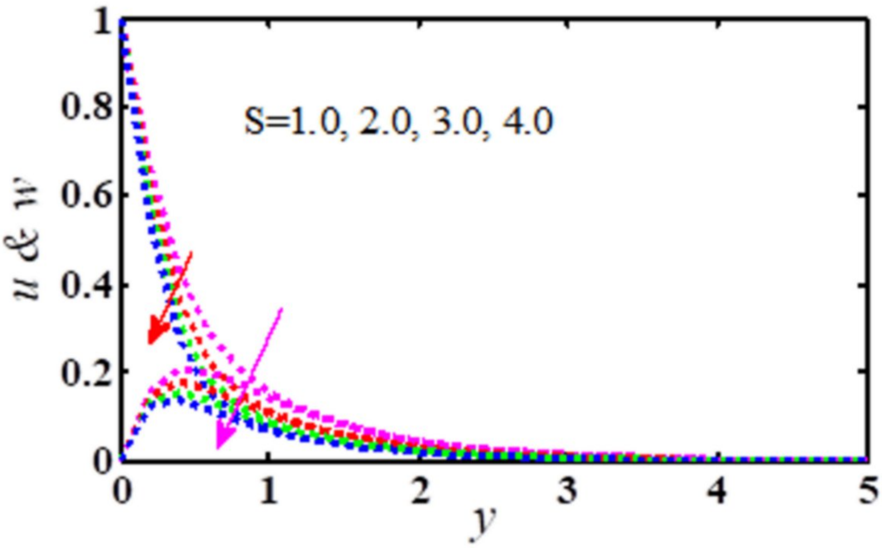

FIGURE 2: Velocity for disparate values of S

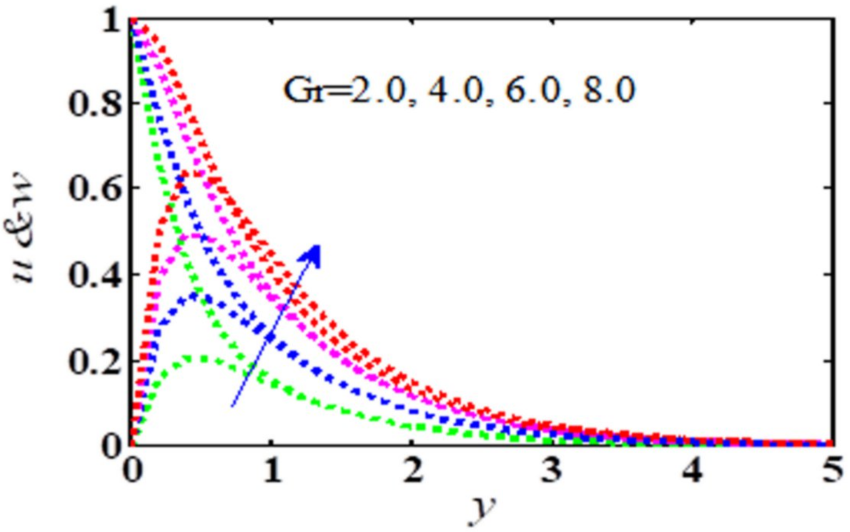

FIGURE 3: Velocity for disparate values of Gr

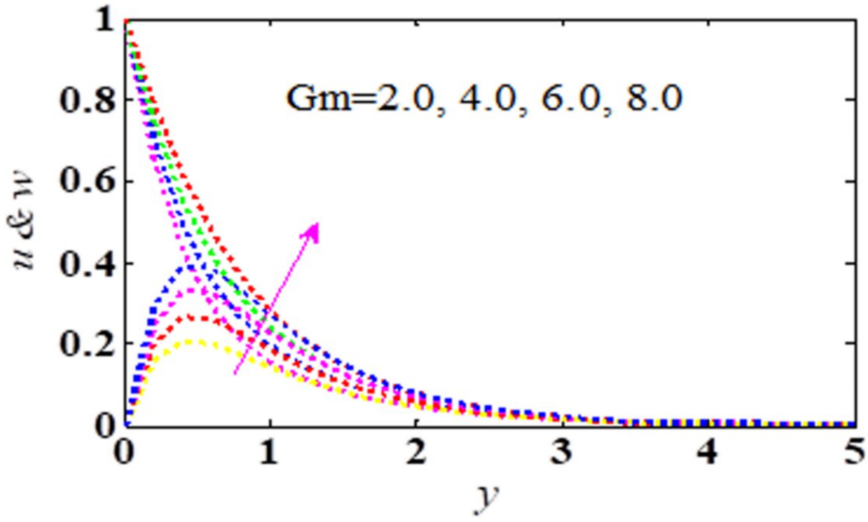

FIGURE 4: Velocity for disparate values of Gm

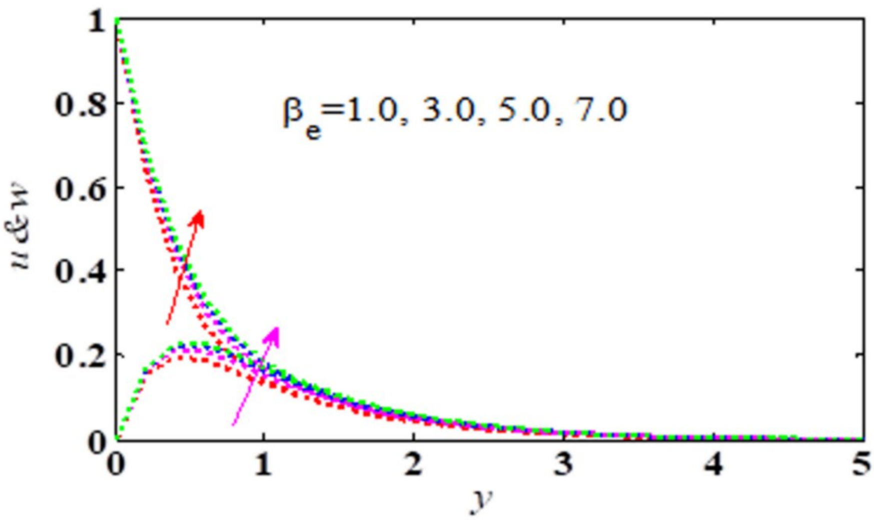

FIGURE 5: Velocity for disparate values of βe

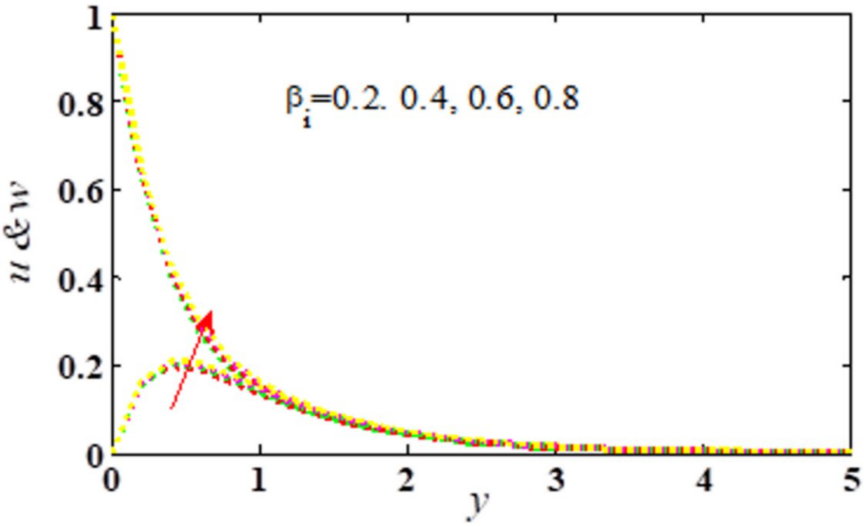

FIGURE 6: Velocity for disparate values of βi

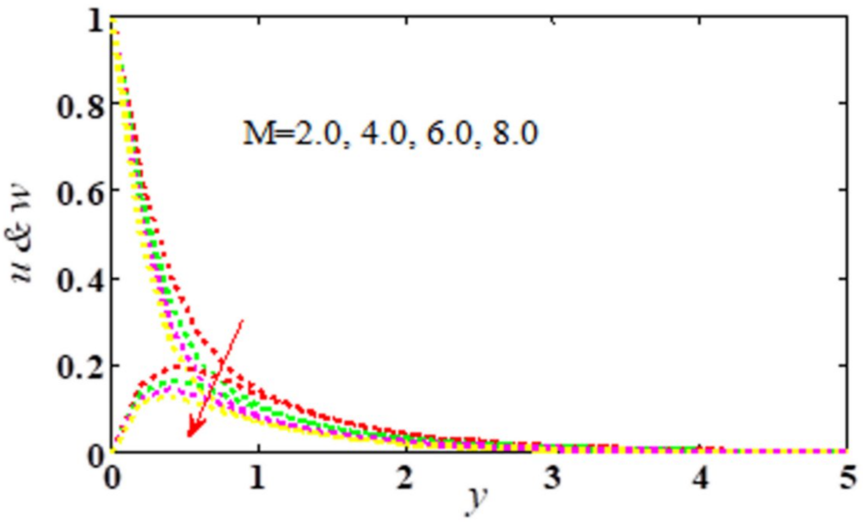

FIGURE 7: Velocity for disparate values of M

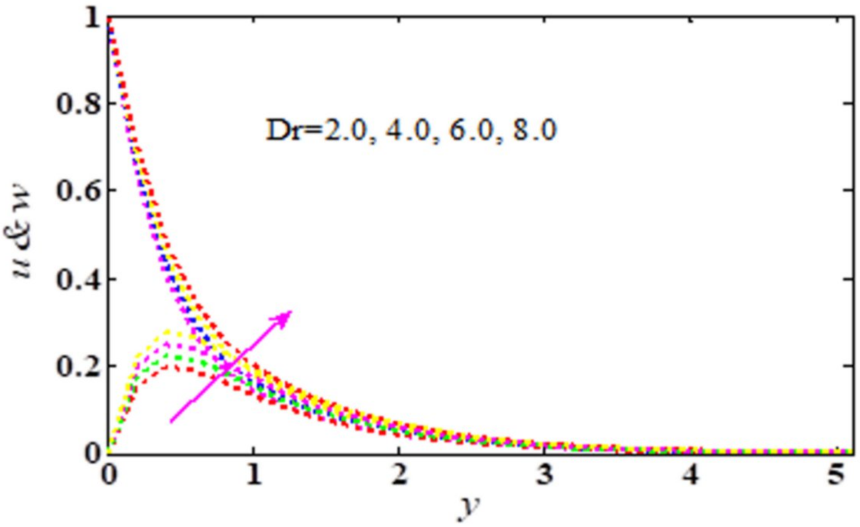

FIGURE 8: Velocity for disparate values of Dr

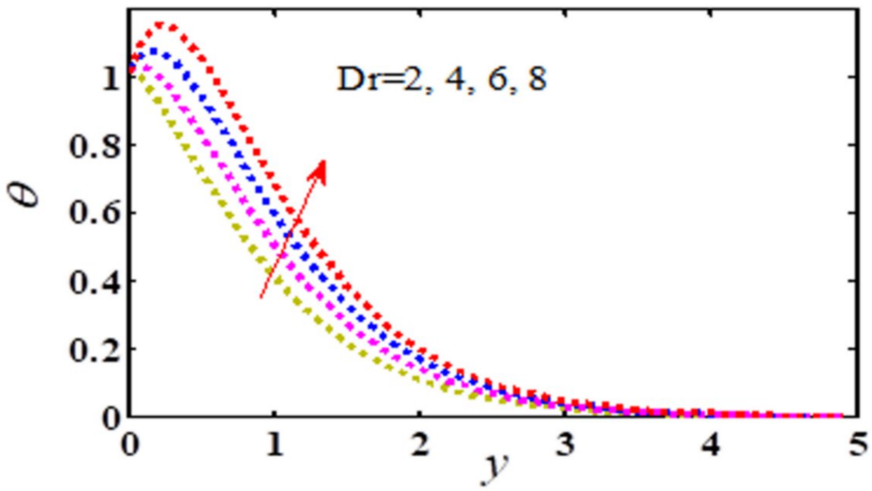

FIGURE 9: Temperature for disparate values of Dr

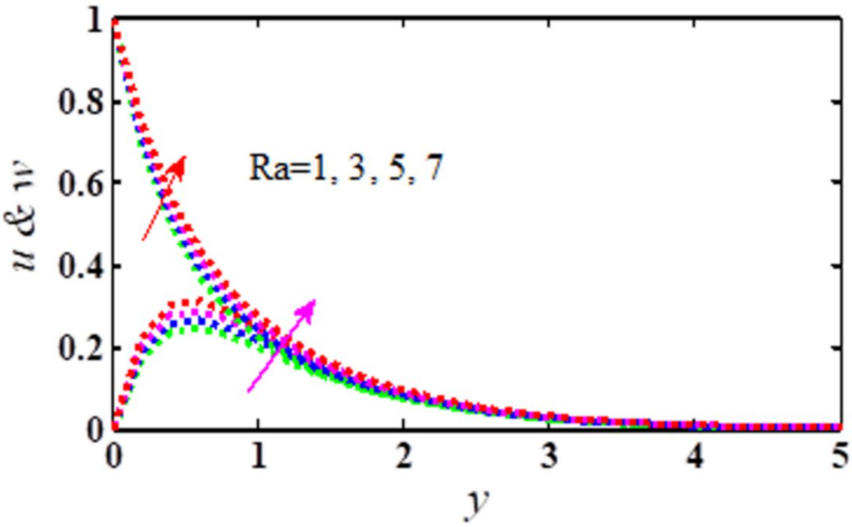

FIGURE 10: Velocity for disparate values of Ra

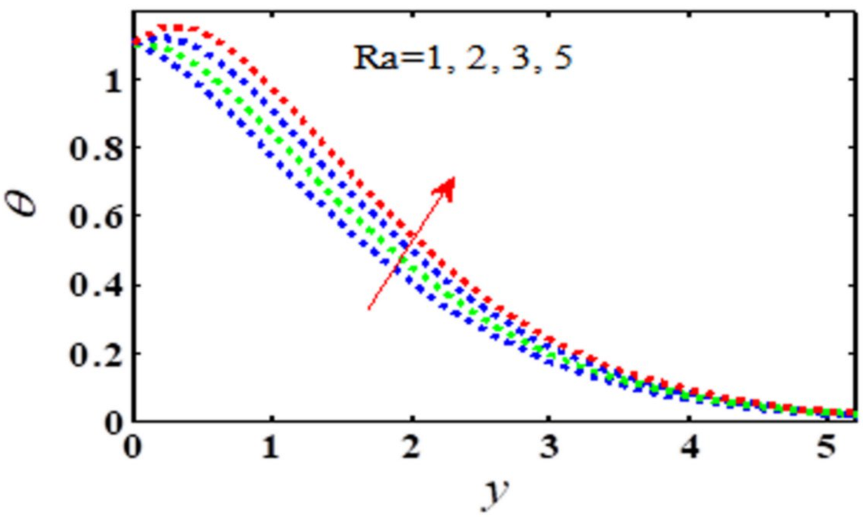

FIGURE 11: Temperature for disparate values of Ra

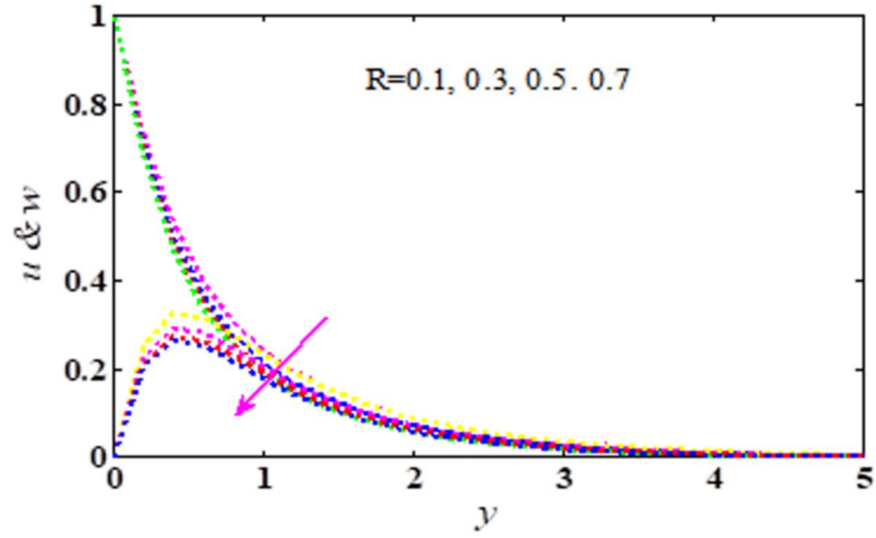

FIGURE 12: Velocity for disparate values of R

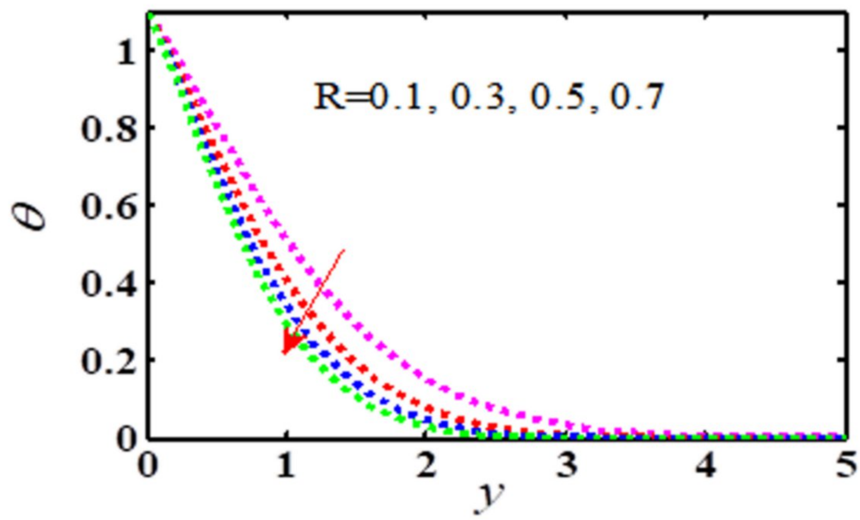

FIGURE 13: Temperature for disparate values of R

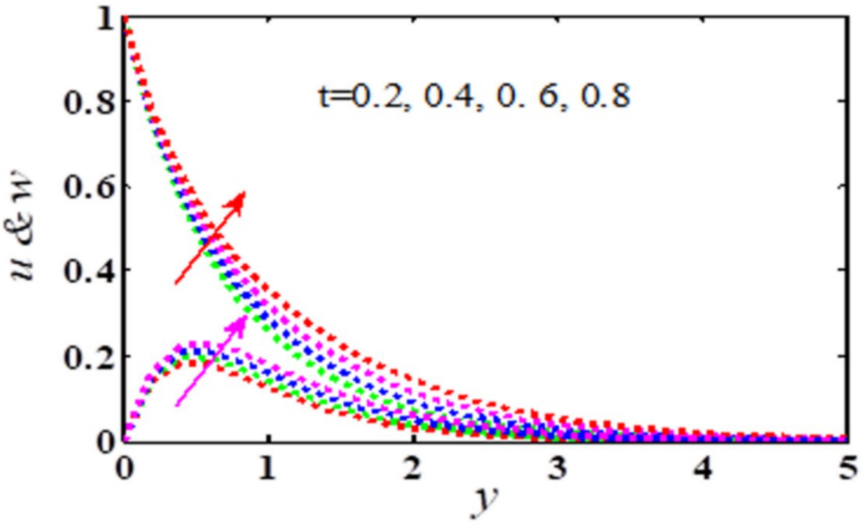

FIGURE 14: Velocity for disparate values of t

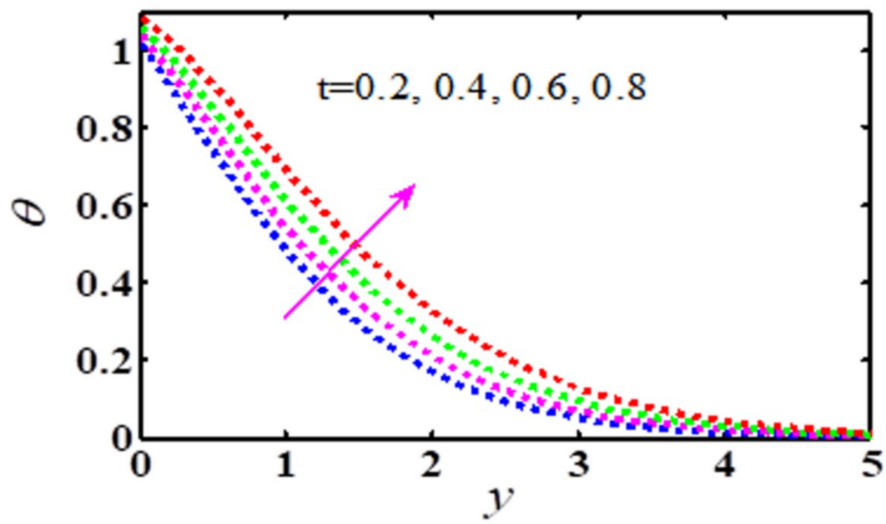

FIGURE 15: Temperature for disparate values of t

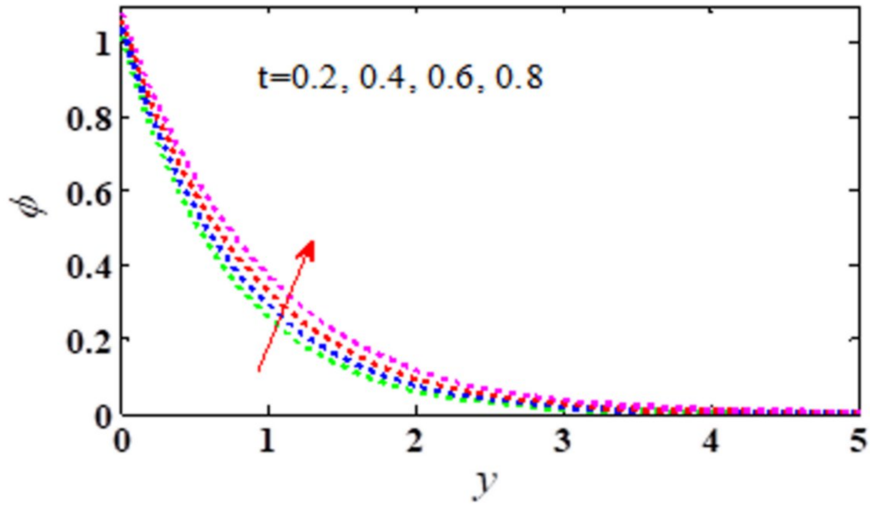

FIGURE 16: Concentration for disparate values of t

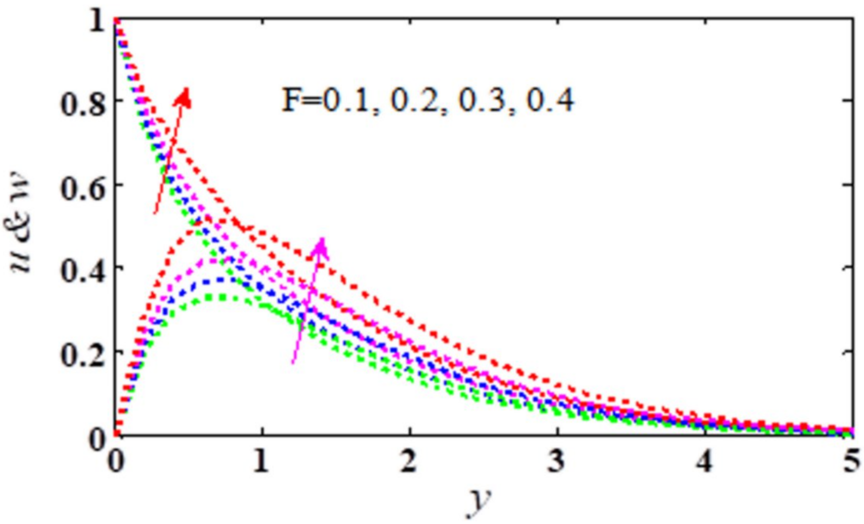

FIGURE 17: Velocity for disparate values of F

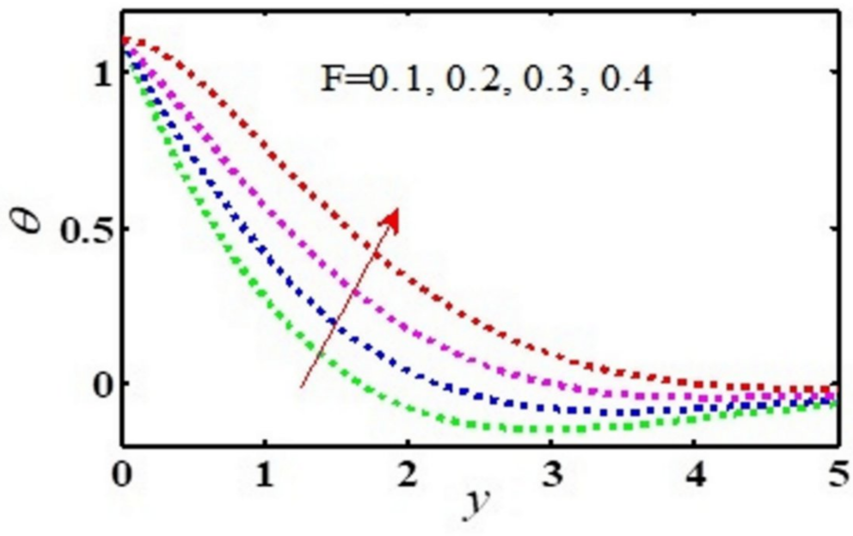

FIGURE 18: Temperature for disparate values of F

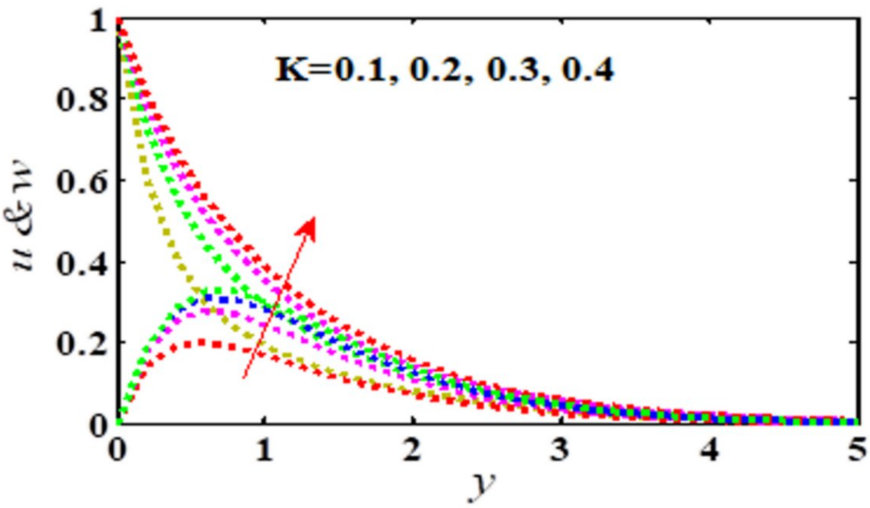

FIGURE 19: Velocity for disparate values of K

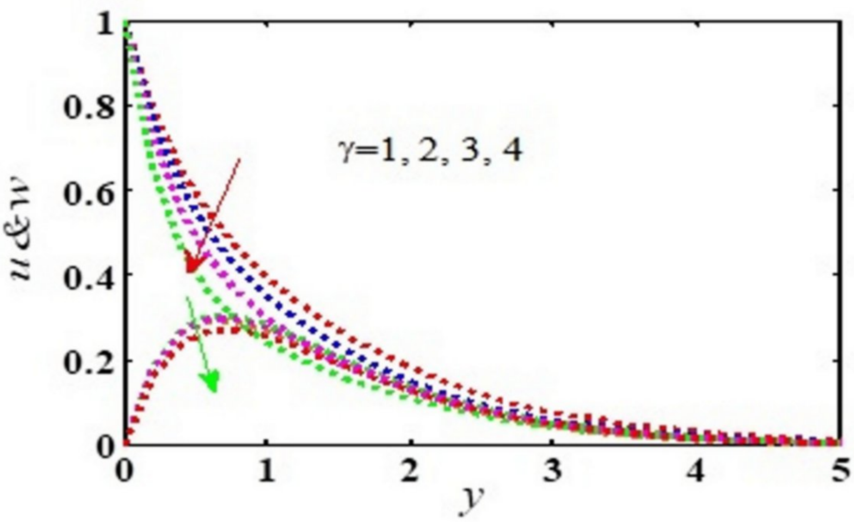

FIGURE 20: Velocity for disparate values of γ

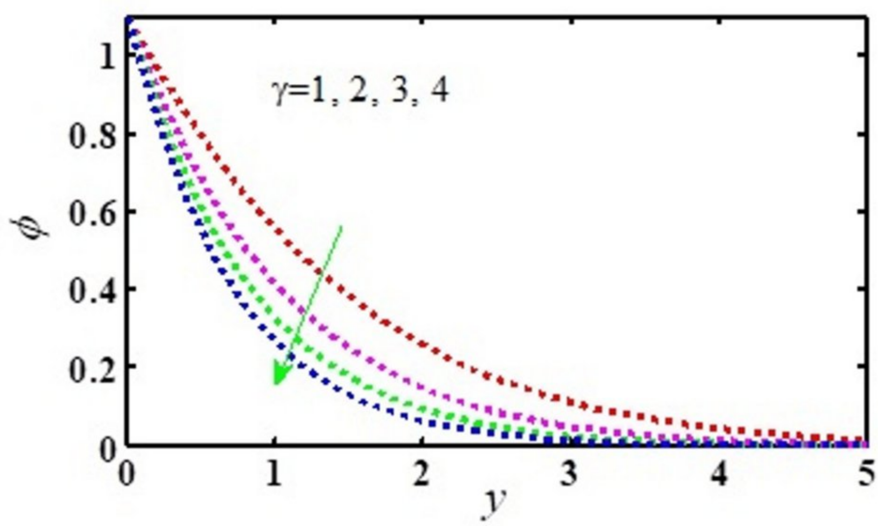

FIGURE 21: Concentration for disparate values of γ

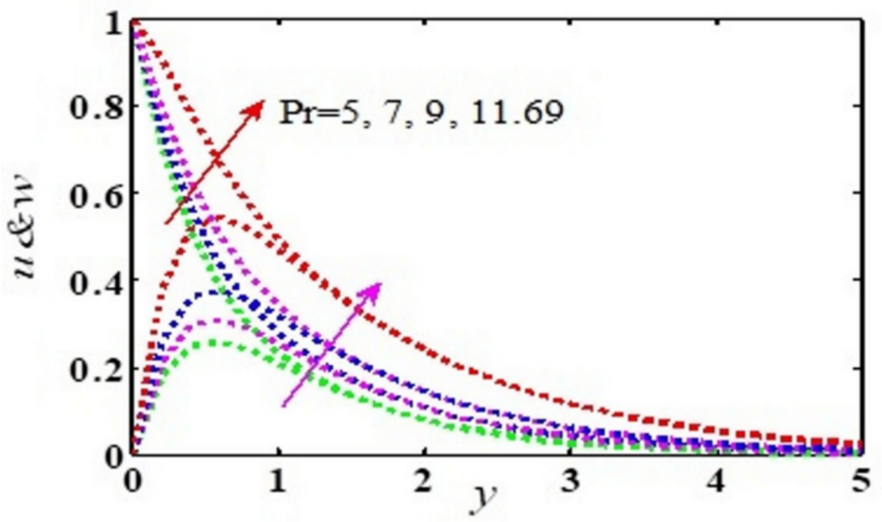

FIGURE 22: Velocity for disparate values of Pr

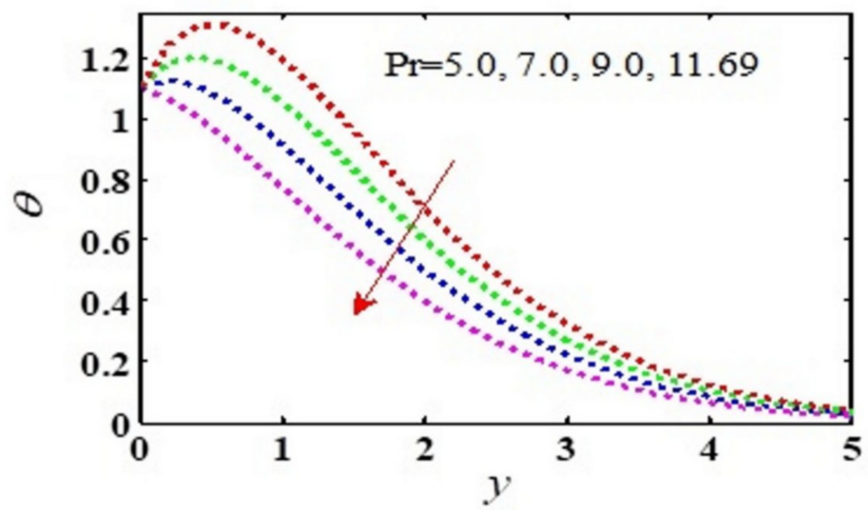

FIGURE 23: Temperature for disparate values of Pr

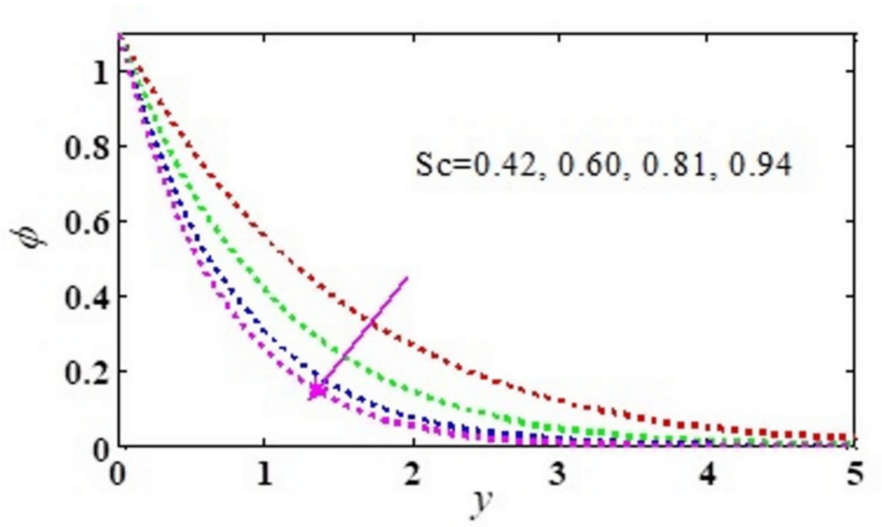

FIGURE 24: Concentration for disparate values of Sc

Pr	β_i	β_e	Gr	Gm	Sc	γ	R	Ra	F	K	S	χ_1	χ_2
5.0	0.2	2.0	2.0	2.0	0.60	2.0	0.1	1.0	0.1	0.2	1.0	8.6177	2.1884
7.0	0.2	2.0	2.0	2.0	0.60	2.0	0.1	1.0	0.1	0.2	1.0	8.6190	2.4065
11.69	0.2	2.0	2.0	2.0	0.60	2.0	0.1	1.0	0.1	0.2	1.0	8.6199	2.4930
7.0	0.4	2.0	2.0	2.0	0.60	2.0	0.1	1.0	0.1	0.2	1.0	8.9823	2.2876
7.0	0.6	2.0	2.0	2.0	0.60	2.0	0.1	1.0	0.1	0.2	1.0	8.8208	2.3796
7.0	0.8	2.0	2.0	2.0	0.60	2.0	0.1	1.0	0.1	0.2	1.0	8.6875	2.4615
7.0	0.2	4.0	2.0	2.0	0.60	2.0	0.1	1.0	0.1	0.2	1.0	8.7505	2.5297
7.0	0.2	6.0	2.0	2.0	0.60	2.0	0.1	1.0	0.1	0.2	1.0	8.5447	2.6679
7.0	0.2	8.0	2.0	2.0	0.60	2.0	0.1	1.0	0.1	0.2	1.0	8.4285	2.7553
7.0	0.2	2.0	4.0	2.0	0.60	2.0	0.1	1.0	0.1	0.2	1.0	9.1875	2.9942
7.0	0.2	2.0	6.0	2.0	0.60	2.0	0.1	1.0	0.1	0.2	1.0	9.2057	3.6901
7.0	0.2	2.0	8.0	2.0	0.60	2.0	0.1	1.0	0.1	0.2	1.0	9.2239	4.3860
7.0	0.2	2.0	2.0	4.0	0.60	2.0	0.1	1.0	0.1	0.2	1.0	9.1918	2.2983
7.0	0.2	2.0	2.0	6.0	0.60	2.0	0.1	1.0	0.1	0.2	1.0	9.2144	3.0995
7.0	0.2	2.0	2.0	8.0	0.60	2.0	0.1	1.0	0.1	0.2	1.0	9.2369	3.9006
7.0	0.2	2.0	2.0	2.0	0.42	2.0	0.1	1.0	0.1	0.2	1.0	9.1739	2.4624
7.0	0.2	2.0	2.0	2.0	0.60	2.0	0.1	1.0	0.1	0.2	1.0	9.1693	2.2983
7.0	0.2	2.0	2.0	2.0	0.84	2.0	0.1	1.0	0.1	0.2	1.0	9.1590	1.9939
7.0	0.2	2.0	2.0	2.0	0.60	4	0.1	1.0	0.1	0.2	1.0	9.1599	2.0175
7.0	0.2	2.0	2.0	2.0	0.60	6	0.1	1.0	0.1	0.2	1.0	9.1458	1.6679
7.0	0.2	2.0	2.0	2.0	0.60	8	0.1	1.0	0.1	0.2	1.0	9.1243	1.2321
7.0	0.2	2.0	2.0	2.0	0.60	2.0	0.2	1.0	0.1	0.2	1.0	9.1702	2.2952
7.0	0.2	2.0	2.0	2.0	0.60	2.0	0.3	1.0	0.1	0.2	1.0	9.1701	2.2921
7.0	0.2	2.0	2.0	2.0	0.60	2.0	0.4	1.0	0.1	0.2	1.0	9.1700	2.2887

7.0	0.2	2.0	2.0	2.0	0.60	2.0	0.1	2	0.1	0.2	1.0	9.1686	2.2748
7.0	0.2	2.0	2.0	2.0	0.60	2.0	0.1	3	0.1	0.2	1.0	9.1679	2.2513
7.0	0.2	2.0	2.0	2.0	0.60	2.0	0.1	4	0.1	0.2	1.0	9.1671	2.2278
7.0	0.2	2.0	2.0	2.0	0.60	2.0	0.1	1.0	0.2	0.2	1.0	9.1686	2.2982
7.0	0.2	2.0	2.0	2.0	0.60	2.0	0.1	1.0	0.3	0.2	1.0	9.1676	2.2981
7.0	0.2	2.0	2.0	2.0	0.60	2.0	0.1	1.0	0.4	0.2	1.0	9.1664	2.2980
7.0	0.2	2.0	2.0	2.0	0.60	2.0	0.1	1.0	0.1	0.1	1.0	9.3246	2.2608
7.0	0.2	2.0	2.0	2.0	0.60	2.0	0.1	1.0	0.1	0.3	1.0	9.1169	2.3109
7.0	0.2	2.0	2.0	2.0	0.60	2.0	0.1	1.0	0.1	0.5	1.0	9.0748	2.3214
7.0	0.2	2.0	2.0	2.0	0.60	2.0	0.1	1.0	0.1	0.2	2.0	9.4303	1.7847
7.0	0.2	2.0	2.0	2.0	0.60	2.0	0.1	1.0	0.1	0.2	3.0	9.1693	1.6279
7.0	0.2	2.0	2.0	2.0	0.60	2.0	0.1	1.0	0.1	0.2	4.0	9.1563	1.5067

TABLE 1: Variation of skin friction for various physical parameters, when Rivlin-Ericksen fluid parameter k1 = 1 and M = 2

Dr	Ra	R	Pr	F	N_w
4	1	0.1	11.69	0.1	-25.7174
6	1	0.1	11.69	0.1	-35.0689
8	1	0.1	11.69	0.1	-44.4204
2	2	0.1	11.69	0.1	-17.9313
2	3	0.1	11.69	0.1	-19.4967
2	4	0.1	11.69	0.1	-21.0620
2	1	0.2	11.69	0.1	-14.3069
2	1	0.3	11.69	0.1	-14.3982
2	1	0.4	11.69	0.1	-14.4916
2	1	0.1	7.00	0.1	-29.7582
2	1	0.1	9.00	0.1	-17.7434
2	1	0.1	11.69	0.1	-16.3659
2	1	0.1	11.69	0.2	-14.9804
2	1	0.1	11.69	03	-15.4152
2	1	0.1	11.69	0.4	-15.8892

TABLE 2: Variation of heat transfer coefficient for varies physical parameters

γ	Sc	S_h
2	0.60	2.2041
3	0.60	3.2124
4	0.60	5.7702
1	0.60	5.7702
1	0.84	6.2608
1	0.94	7.0826

TABLE 3: Variation of mass transfer coefficient for varies physical parameters

Discussion

This paper aims to meticulously examine the impact of rotating Rivlin-Ericksen fluid model, Hall effect and ion-slip current on MHD flow past an impulsively started infinite vertical plate embedded in a porous medium with chemical reaction. The objective is to gain a comprehensive understanding of how various flow parameters influence the discussed flow problem.

Figure *2* exhibited that axial and transverse components of velocities varied with heterogeneous progressive values of the angle of rotation (S). In the perspective of the Rivlin-Ericksen fluid model (REFM), the relationship between velocity as well as the angle of rotation can be influenced by the rheological properties of the fluid. The REFM describes the demeanor of non-Newtonian fluids, which have complex viscosity properties that can vary with shear rate, shear stress, or other factors. In such a model, from the figure, it is observed that both axial and transverse components of velocity decrease with increasing values of the angle of rotation. It could be due to the shear-thinning comportment of the fluid. Shear thinning refers to the property of certain non-Newtonian fluids where their viscosity decreases as the shear rate (or angular velocity, in the context of rotation) increases.

The influence of the Grashof number (Gr) on axial and transverse velocities was depicted in Figure *3*. Gr is a dimensionless parameter in fluid dynamics, comparing buoyancy to viscosity effects, particularly relevant in natural convection. In the context of a REFM, both velocities increased with rising Gr, indicating stronger buoyancy-driven flow. REFM represents a non-Newtonian fluid, exhibiting complex deeds not following linear stress-strain rate relations, with viscosity varying under shear. Higher Gr could intensify buoyancy-driven flow and temperature differences in non-Newtonian fluids, potentially resulting in increased velocities. However, the relationship between velocity, Gr, and REFM performance is intricate and influenced by multiple factors.

Increasing the Solutal Grashof number (Gm) signifies a greater influence of concentration-driven buoyancy forces relative to viscous forces in non-Newtonian fluids, leading to heightened fluid motion and potentially complex changes in velocity due to the interplay between concentration-driven buoyancy and non-Newtonian behavior as was shown in the Figure *4*.

The significance of Hall current effect (βe) on both velocity profiles was shown in Figure *5*. This figure contemplates that both velocity increases with enhance in the Hall current within the REFM; it suggests a unique deeds of the fluid under the influence of the Hall current. This behavior might be a result of the intricate interactions between the non-Newtonian properties of the fluid described by the REFM and the additional forces introduced by the Hall current. Here are a few possible reasons why this conduct might occur, i.e., the Hall current introduces magnetic forces that interact with the fluid's flow behavior. This interaction could lead to changes in the fluid's microstructure, viscosity, or elastic properties, causing an increase in both velocities. An increase in the Hall current could potentially enhance this shear-thinning behavior, resulting in higher velocities at higher current values. Moreover, depending on the specific characteristics of the fluid and the Hall current, electromagnetic effects could play a role in altering the fluid's deeds and increasing velocity.

An emphasis on the ion-slip effect on both velocities is shown in Figure *6*: When discussing the velocity of a fluid, the ion slip effect can play a significant role, especially in cases involving charged particles or ions. Ion slip refers to the relative motion between ions and the surrounding fluid in an electric field. This effect is particularly important when dealing with ion-containing fluids, such as electrolytes or ionized gases. When an electric field is applied to such a fluid, the ions will experience forces that can influence their motion and interact with the fluid's velocity field. In the approach of the REFM, if the liquid contains ions and is subjected to an electric field, the ion slip effect can lead to changes in the fluid's velocity. The ions' motion, driven by the electric field, can affect the overall momentum and flow mien of the fluid. As the ion slip effect becomes more pronounced, both fluid's velocities increase, especially in regions where ion concentration gradients or electric fields are significant. It's worth noting that the exact ongoing of a fluid under the REFM, including the effects of ion slip, can be complex and depend on various factors such as the fluid's rheological properties, the strength of the electric field, and the geometry of the system. Analyzing and predicting the demeanor of such fluids often requires solving intricate mathematical equations derived from the model.

Figure *7* shows impact of magnetic field (M) on both velocities. In the presence of a magnetic field, the mien of a fluid can be described by MHD principles. The interaction between the fluid's motion and the magnetic field can lead to changes in the fluid's velocity and flow patterns. One of the key effects of a magnetic field on a fluid is the creation of Lorentz forces, which act perpendicular to both the fluid's velocity and the magnetic field direction. In the case where a magnetic field is applied to a REFM, the Lorentz forces can potentially oppose or diminish the fluid's velocity. This is because the Lorentz forces exerted on the fluid can counteract the forces driving the fluid's motion, leading to a reduction in the overall velocity of the fluid. The exact impact of the magnetic field on the fluid's velocity will depend on factors such as the strength and orientation of the magnetic field, the rheological properties of the fluid, and the specific geometry of the system. It's important to note that the interaction between a magnetic field and a viscoelastic fluid under the Rivlin-Ericksen model can be quite complex and may involve solving intricate mathematical equations.

Figures *8* and 9 portrayed influence of Dufour effect on both velocities as well as temperature. The Dufour effect involves the coupling between concentration gradients and temperature gradients. When discussing the impact of the Dufour effect on velocity and temperature in the context of the REFM, several considerations come into play; the Dufour effect can influence the velocity of a Rivlin-Ericksen fluid through induced convection. As concentration gradients lead to temperature gradients due to the Dufour effect, regions with differing temperatures can result in fluid motion. In a viscoelastic fluid described by the Rivlin-Ericksen model, this fluid motion can interact with the material's elastic properties, potentially affecting the overall velocity of the fluid. The enhancement of the Dufour effect could lead to stronger concentration-induced temperature gradients, which in turn might lead to increased convective motion and, consequently, higher fluid velocities. Meanwhile, in the Rivlin-Ericksen model, the Dufour effect could lead to temperature variations within the fluid due to the coupling between concentration and temperature. As the Dufour effect is enhanced, the temperature gradients induced by concentration gradients can become more pronounced. This can result in regions of increased temperature within the fluid. It is important to emphasize that the interplay between the Dufour effect and the convoluted manners of a viscoelastic fluid described by the Rivlin-Ericksen model can lead to intricate and non-linear effects.

Figure *10* represents effect of both velocities with the various incremental values of Radiation absorption. Radiation can transfer energy to an object upon absorption. This is seen in various phenomena, such as the photoelectric effect, where photons (particles of light) transfer energy to electrons, causing them to be emitted from a material. The key idea is that absorbed radiation can lead to an increase in the internal energy of the object, which can then manifest as an increase in velocity. When the radiation absorption parameter "Ra" increases, it implies that the material or object in question is more efficient at absorbing radiation. This could be due to factors such as the material's properties, surface area, or other characteristics. As "Ra" increases, the object absorbs more energy from the radiation. The absorbed energy from the radiation is converted into kinetic energy of the object's constituent particles. In classical mechanics, the kinetic energy of an object is directly proportional to its velocity squared. Therefore, as the object absorbs more energy and its internal kinetic energy increases, the object's velocity can also increase. In some cases, absorbed radiation can lead to a rise in temperature. This increase in temperature can cause the particles within the object to move faster and, consequently, increase the object's overall velocity. When radiation is absorbed, it can also exert a pressure on the object's surface. This pressure difference can lead to an increase in velocity. The absorbed radiation can also transfer momentum to the object, contributing to its motion and velocity.

Influence of Radiation absorption on temperature was shown in the Figure *11*. The increase in temperature with rising values of radiation absorption is a fundamental concept in physics and can be explained using the principles of thermodynamics and the interaction between radiation and matter. When radiation is absorbed by a material, its energy is transferred to the material's constituent particles, typically atoms or molecules. This energy is distributed among the particles as increased kinetic energy, which causes them to move more vigorously. This increased motion at the microscopic level translates to an increase in the material's temperature at the macroscopic level. Here's why this happens: When electromagnetic radiation (such as light or other forms of radiation) interacts with matter, its energy can be transferred to the material. The energy of radiation is quantized in discrete packets called photons. When radiation is absorbed, the energy of the absorbed photons is distributed among the particles, increasing their kinetic energy. The particles move more vigorously, which corresponds to an increase in temperature. It is important to note that the relationship between absorbed energy, temperature increase, and the specific material properties can be complex and may vary depending on factors such as the material's composition, density, and heat capacity.

Figures 12 and 13 indicate variations of primary as well as secondary velocities with the effect of radiation parameter (R). Velocity and temperature reduced with the increasing values of radiation parameter (R). From this, there is a relationship between a radiation parameter and the velocity and temperature of a system. Radiation can exert a force on a material, known as radiation pressure. This force can act in the direction opposite to the fluid flow or motion, causing a reduction in velocity. If the radiation parameter is related to the intensity or energy of radiation, an increase in this parameter might result in stronger radiation pressure, leading to a decrease in velocity. Meanwhile radiation can also lead to cooling effects. In certain situations, high-energy radiation can cause energy to be lost from a material, leading to a decrease in its temperature. If the radiation parameter represents the energy or intensity of the radiation, an increase in this parameter might correspond to more cooling effects, resulting in a temperature reduction. Radiation is a mode of heat transfer.

Velocity, temperature, as well as concentration increase with the incremental values of time (t) in the case of the Rivlin-Ericksen fluid model was illustrated in Figures 14, 15, and 16. Velocity increase with Time (t): in fluid dynamics, the velocity of a fluid element can change over time due to various factors, such as external forces, pressure gradients, and flow conditions. In the case of the Rivlin-Ericksen fluid model, if the velocity of the fluid increases with incremental values of time (t), it could be due to changes in applied forces, boundary conditions, or other factors influencing the fluid flow. Non-Newtonian fluids like those described by the Rivlin-Ericksen model can exhibit complex behaviors, and the specific relationship between velocity and time would depend on the model parameters and the nature of the flow. Temperature Increase with Time (t): An increase in temperature with time could be due to factors such as heat generation, heat conduction, or external heat sources. In some cases, the increase in temperature could lead to changes in the fluid properties, such as viscosity and density, which, in turn, could affect the fluid's behavior. The Rivlin-Ericksen fluid model might account for such temperature-related effects and their impact on the fluid's characteristics. Concentration Increase with Time (t): An increase in concentration with time could indicate processes such as diffusion, convection, or chemical reactions within the fluid. For instance, if a solute is introduced into the fluid and its concentration increases over time, this could be due to the diffusion of the solute particles through the fluid. The Rivlin-Ericksen fluid model may include terms or equations that describe how concentration changes within the fluid, considering its non-Newtonian behavior.

Influence of the heat source parameter (F) on both velocities was revealed in Figure 17. In heat transfer, when it is observed that there is a strengthening in velocity with augmenting values of a heat source parameter, it generally indicates a convective heat transfer process. Convective heat transfer involves the transfer of heat between a fluid (liquid or gas) and a solid surface due to the fluid's movement or circulation. This process occurs because the fluid near the heated surface gets hotter, becomes less dense, and tends to rise. As it moves away from the heated surface, cooler fluid replaces it, creating a circulation pattern known as convection currents. When the heat source parameter is increased (which often means increasing the temperature difference between the fluid and the heated surface), the fluid near the heated surface becomes hotter. This leads to a higher temperature gradient between the fluid and the surface. As the fluid near the heated surface gets hotter, its density decreases. A decrease in density makes the fluid buoyant, causing it to rise. In addition, the rising hot fluid creates a convection current. Cooler fluid from other parts of the system moves in to replace the rising fluid. This circulation of fluid creates movement, which is manifested as an increase in both velocities. Finally, an increase in the heat source parameter leads to a stronger temperature gradient, more buoyant fluid, and more pronounced convection currents. This increased circulation results in higher fluid velocities near the heated surface.

Figure 18 reflects the impact of heat source parameter (F) on temperature. From the figure, it is noticed that an escalation in the heat source parameter is leading to an intensification in temperature. This relationship is a common occurrence in many physical systems. When a heat source parameter is expanded, it typically results in more energy being introduced into the system, which leads to strengthening in the average kinetic energy of the particles within the system. This increase in kinetic energy translates to higher temperatures. For instance, consider a simple system like a pot of water on a stove. When it turns up the heat (increase the heat source parameter), the burner emits more heat energy into the water. This additional energy causes the water molecules to move more rapidly, leading to an increase in temperature. In more complex systems, such as in physics, chemistry, and engineering, this relationship between a heat source parameter and temperature is described by various equations and principles, such as the laws of thermodynamics. The exact nature of the relationship can depend on the specific properties and characteristics of the system under consideration.

Both velocity components increase with increasing values of the porous medium (K) as illustrated in the Figure 19. The parameter K could represent the permeability of the porous medium. Permeability is a fundamental property of porous media that measures how easily fluids can flow through the medium. It quantifies the ability of a porous material to transmit fluids (liquids or gases) under the influence of a pressure gradient. Higher permeability means that fluids can flow more easily through the porous medium. When permeability "K" increases, it generally leads to higher fluid flow rates or velocities through the porous medium. This relationship can be understood through Darcy's law, which relates the flow rate of a fluid through a porous medium to the permeability, pressure gradient, and cross-sectional area of the medium. This relationship has significant implications for various fields such as groundwater hydrology, petroleum reservoir engineering, and filtration processes. Key points to consider when "K" increases and velocity increases: Higher permeability means there is less resistance to fluid flow within the porous medium. As a result, the fluid can move more easily through the medium, leading to an increase in velocity. With increased permeability, larger volumes of fluid can pass through the porous medium in a given amount of time, resulting in higher flow rates and velocities. In addition, the relationship described by Darcy's law suggests that as permeability increases, the pressure gradient can drive a higher flow rate, resulting in increased velocity.

Figures *20* and 21 demonstrated the significance of chemical reaction on both velocities and concentration. Form these figures, both velocities and concentration declined with the effect of chemical reaction parameter. It suggests that the presence of a chemical reaction has a significant influence on both the velocity and the concentration of a fluid. Chemical reactions can release or absorb energy, which can affect the fluid dynamics of a system. If the chemical reaction is exothermic (releases heat) or endothermic (absorbs heat), it can lead to changes in temperature. These temperature changes can, in turn, affect the fluid's viscosity, density, and other properties that influence its velocity. An increase in viscosity can lead to a decline in fluid velocity due to increased internal friction. Additionally, chemical reactions might produce reaction products that influence the overall flow nature, causing a decrease in velocity. Chemical reactions involve the conversion of reactants into products, which can result in changes in the concentration of various species within the fluid. If the reaction involves the consumption or production of species that directly influence the concentration of other species, it can lead to concentration changes. For instance, if a reactant is consumed in the reaction, its concentration will decrease over time. These concentration changes can also affect fluid properties, such as viscosity or density, which can further impact the fluid dynamics.

Figure *22* indicates consequences of both velocities profiles for dissimilar estimators of the Prandtl number. The Prandtl number (Pr) is a dimensionless number that relates the momentum diffusivity (viscosity) of a fluid to its thermal diffusivity. It is often used in the study of heat transfer and fluid dynamics. From the figure, it is clearly explored that axial and transverse components of velocities are enhanced with the various augmented values of Pr. Due to this, when considering the manners of velocity in relation to the Prandtl number, it's important to understand that the Prandtl number primarily affects the relative rates of momentum diffusion and thermal diffusion within a fluid. This, in turn, can impact the overall flow and heat transfer characteristics of the fluid. In natural convection scenarios (such as fluid motion due to temperature differences), the deeds can be more complex. Generally, a higher Prandtl number can lead to increased buoyancy effects, which in turn can influence the velocity patterns. The flow behavior and heat transfer in these situations may be affected by the competition between thermal diffusion and momentum diffusion, with different Prandtl numbers leading to different dominant mechanisms. Finally, the increase in velocity with an increase in the Prandtl number is a consequence of the interplay between momentum diffusion and thermal diffusion, and it can have significant implications for the manners of fluids in various heat transfer and fluid dynamics scenarios.

Figure *23* represents temperature profile with the various accelerated values of Prandtl number (Pr) in the context of secondary grade fluid. The Prandtl number (Pr) is a dimensionless number that represents the ratio of momentum diffusivity (kinematic viscosity) to thermal diffusivity in a fluid. In fluid dynamics and heat transfer, the Prandtl number plays a role in determining how heat is transferred within a fluid compared to how momentum is transferred. A higher Prandtl number indicates that the fluid's thermal diffusivity is relatively greater compared to its kinematic viscosity. This means that heat is transferred more slowly within the fluid compared to the transfer of momentum. In practical terms, fluids with higher Prandtl numbers tend to have thicker thermal boundary layers and thinner momentum boundary layers. Now, it is observed that temperature decreases with increasing Prandtl number, so it is important to consider the specific context and conditions of the fluid flow. When the Prandtl number is higher, it indicates that thermal diffusivity is relatively more important than momentum diffusivity. In such cases, heat is transported more slowly compared to momentum, which could lead to temperature decreases as the heat transfer rate becomes slower. In certain fluid flows, changes in the Prandtl number can affect the velocity and temperature profiles differently. If the fluid has a high Prandtl number, it might influence the temperature distribution more than the velocity distribution, leading to temperature decreases. The deeds of temperature with respect to the Prandtl number could also be influenced by boundary conditions, the presence of heat sources or sinks, or other external factors affecting the heat transfer process.

Figure *24* specifies impact of Schmidt number on both velocities in presence of Rivlin-Ericksen fluid model. The relationship between concentration and the Schmidt (Sc) number is an important concept in fluid dynamics and mass transfer processes, particularly in the context of diffusion and convective transport. The Schmidt number relates the relative importance of momentum diffusion (viscous effects) to mass diffusion in a fluid. The Schmidt number essentially characterizes how easily mass can diffuse through a fluid compared to how momentum diffuses. A higher Sc number implies that momentum diffuses more readily than mass, while a lower Sc number indicates that mass diffusion is more dominant. where concentration diminishes with increasing values of the Schmidt number (Sc), it means that as the importance of momentum diffusion increases relative to mass diffusion (higher Sc), the ability of the substance to disperse or diffuse through the fluid decreases. This could be due to increased resistance from the fluid's viscosity, which hampers the movement and spread of the substance. In practical terms, this relationship can be observed in various situations involving mass transfer: In convective transport, where both convection (bulk fluid movement) and diffusion play a role in mass transfer, a higher Schmidt number can result in reduced mass transfer rates due to the dominance of momentum diffusion over mass diffusion.

Table *1* demonstrated that influence of various parameters which were mentioned in the governing equations. From the table it was observed that an increase in Pr indicates that heat diffuses more slowly compared to momentum. This could potentially lead to reduced thermal boundary layer thickness, resulting in increased fluid velocities near the surface. Higher fluid velocities can lead to increased skin friction of primary and secondary velocities due to enhanced momentum transfer at the boundary layer. Meanwhile an increase in Gr generally implies stronger buoyancy-driven fluid motion, which can result in thicker boundary layers and more vigorous flow near the surface. This increased flow can contribute to higher skin friction of primary and secondary velocities. Similar to the Gr, an increase in Gm indicates stronger buoyancy-driven mass transfer and fluid motion due to concentration differences. This can lead to thicker concentration boundary layers and potentially increased skin friction of both velocities. In addition, The Schmidt number (Sc) is a dimensionless quantity that represents the ratio of momentum diffusivity to mass diffusivity. In fluid dynamics, it is often used to characterize the relative importance of momentum and mass transfer in a fluid. A higher Schmidt number generally indicates lower rates of mass transfer and, consequently, could lead to reduced skin friction. These terms are likely related to heat transfer through radiation. An increase in the radiation parameter(R) or radiation absorption could enhance heat transfer away from the surface, potentially reducing skin friction. An increased heat source might lead to changes in temperature gradients near the surface, which could impact the fluid flow behavior and potentially influence skin friction. Viscoelasticity (γ) refers to a material's combination of viscous (fluid-like) and elastic (solid-like) properties. A change in the viscoelastic parameter could alter the flow behavior of the fluid near the surface and, consequently, affect skin friction. This likely refers to the permeability (represented by K) of a porous medium through which the fluid is flowing. Changes in permeability can influence the flow pattern and affect skin friction. Angular rotation (S) could refer to the angular velocity or rotational motion of the solid surface. This motion could potentially impact the flow characteristics and skin friction. Besides, the increasing values of Hall and ion slip current leads to decline in skin friction of primary velocity, but considerable enhancement was obtained in case of secondary velocity of skin friction. Table *2* represents significance of various parameters related to coefficient of heat transform. From the table it was establish that Nusselt number diminished with effect of Dr, Ra R as well as F, but in case of Pr, the Nusselt number enhanced. Meanwhile, Table *3* illustrated that influence of chemical reaction (γ) and Schmidt number (Sc) on the Sherwood number. From the table, it was revealed that an increase in the Sherwood number occurs with both incremental values of the chemical reaction rate and Schmidt number. It suggests that both the increased chemical reaction rate and the change in species diffusivity due to a higher Schmidt number are positively impacting the mass transfer process. This would result in more efficient transfer of species across the interface, leading to an enhancement in the Sherwood number.

Validity of the study

The study compared its findings to previous research by Rajakumar et al. [13]. regarding skin friction when the rotational parameter S is zero. The impact of both skin frictions with the influence of M was reported in Table *4*. It highlighted the significant attention garnered by the influence of a magnetic field on skin friction in various engineering and scientific applications. The introduction of a magnetic field, termed magnetohydrodynamic (MHD) enhancement, was found to notably increase skin friction along the primary velocity component due to increased momentum transfer from magnetic forces. However, a counter-effect was observed in the secondary velocity component, where skin friction decreased due to altered flow patterns and reduced momentum transfer caused by the magnetic field.

M	Current results when S = 1		Previous study when S = 0 in [13]		Current results when S = 0	
4	1.0177	2.1014	-0.7967	3.2392	-0.7967	3.2392
6	1.1091	1.8910	-0.3079	4.5198	-0.3079	4.5198
8	1.1932	1.7347	-0.2190	5.8004	-0.2190	5.8004

TABLE 4: Comparison of both skin frictions with magnetic field (M), when Rivlin-Ericksen fluid parameter k1 = 1

Conclusions

In summary, this research delved into the intricacies of MHD rotating Rivlin-Ericksen fluid flow past an impulsively started infinite vertical porous plate, considering the interplay of various influential factors such as radiation absorption, chemical reactions, and ion slip current effects. Through rigorous analysis using the perturbation method, several key conclusions were drawn:

Influence of Angle of Rotation (S), Magnetic Field (M), Grashof Number (Gr), and Solutal Grashof Number (Gm). This behavior is crucial in MHD cooling systems, such as in nuclear reactors or electronic device cooling, where controlling rotation and magnetic fields can help modulate flow behavior. Additionally, in meteorology or oceanography, understanding how buoyancy-driven flows respond to thermal and solutal gradients can enhance climate and pollution dispersion modeling.

Effect of Hall and Ion-Slip Currents. This result is applicable in plasma dynamics and space propulsion systems (like Hall effect thrusters), where electromagnetic fields influence ionized gases. It is also significant for semiconductor manufacturing or fusion reactor designs, where controlling ionized fluid flow is essential.

Dufour and Radiation Absorption Effects. Such enhancements in velocity and temperature are important in solar energy collectors and combustion chambers, where thermal radiation and cross-diffusion effects (like the Dufour effect) impact efficiency. It also applies in thermal insulation systems where heat and mass transfer processes must be optimized.

Influence of Time (t) on Velocity, Temperature, and Concentration. This conclusion has relevance in transient heat and mass transfer studies, such as start-up conditions in industrial processes, or in environmental systems like pollutant dispersion over time. It can also help in optimizing batch reactors or time-dependent cooling/heating operations.

Chemical Reaction Effects on Velocity and Concentration. This is significant in chemical process engineering, especially in reactive flow systems like catalytic converters or combustion processes. It implies that chemical reactions can slow down fluid motion and reduce reactant concentrations, which is crucial in reaction rate control and efficiency analysis.

Influence of Heat Source Parameter (F) and Prandtl Number (Pr). This behavior is applicable in internal combustion engines, solar thermal systems, and HVAC (Heating, Ventilation, and Air Conditioning) systems where internal heat generation influences performance. Understanding how Prandtl number variations affect temperature and velocity helps in fluid selection for coolants or lubricants.

Influence of Schmidt Number (Sc) and Radiation Parameter (R). These effects are important in mass transfer operations such as drying, evaporation, or absorption systems, where controlling species diffusion is vital. Reduced performance under radiative conditions also applies to thermal shielding, spacecraft insulation, and high-temperature manufacturing processes.

Appendices

$$[m_1 = \frac{Sc + \sqrt{(Sc)^2 + 4Sc\left(\gamma + \frac{i\omega}{4}\right)}}{2}]$$

$$[m_2 = \frac{1 + \sqrt{1 + 4\Gamma\left(-F + \frac{i\omega}{4}\right)}}{2}]$$

$$[m_3 = \frac{1+\sqrt{1+4N}}{2}]$$

$$[h_1 = \left(\frac{-Dr\ m_1^2 - Ra}{\Gamma m_1^2 - m_1 - \left(-F + \frac{i\omega}{4}\right)}\right)]$$

$$[h_2 = \left(\frac{-Gr\ A_0}{m_2^2 - m_2 - N}\right)]$$

$$[h_3 = \left(\frac{-Gr\ N_1\ - Gm}{m_2^2 - m_2 - N}\right)]$$

$$[h_4 = \left(\frac{-\frac{i\omega}{4} m_1^2 N_3\ + m_1^3 N_3}{m_1^2 - m_1 - N}\right)]$$

$$[h_5 = \left(\frac{-\frac{i\omega}{4} m_2^2 N_2\ + m_2^3 N_2}{m_2^2 - m_2 - N}\right)]$$

$$[h_6 = \left(\frac{-\frac{i\omega}{4} m_3^2 A_1\ + m_3^3 A_1}{m_3^2 - m_3 - N}\right)]$$

$$[A_0 = 1 - h_1]$$

$$[A_1 = e^{-i\omega t} - h_2 - h_3]$$

$$[A_1 = -h_6 - h_4 - h_5]$$

Additional Information

Author Contributions

All authors have reviewed the final version to be published and agreed to be accountable for all aspects of the work.

Concept and design: KVB Rajakumar, T Govinda Rao, TRKD Vara Prasad

Acquisition, analysis, or interpretation of data: KVB Rajakumar, G Sreenivasulu, T Govinda Rao, TRKD Vara Prasad

Drafting of the manuscript: KVB Rajakumar, T Govinda Rao, TRKD Vara Prasad

Critical review of the manuscript for important intellectual content: KVB Rajakumar, G Sreenivasulu, T Govinda Rao, TRKD Vara Prasad

Supervision: KVB Rajakumar, T Govinda Rao, TRKD Vara Prasad

Disclosures

Human subjects: All authors have confirmed that this study did not involve human participants or tissue. **Animal subjects:** All authors have confirmed that this study did not involve animal subjects or tissue. **Conflicts of interest:** In compliance with the ICMJE uniform disclosure form, all authors declare the following: **Payment/services info:** All authors have declared that no financial support was received from any organization for the submitted work. **Financial relationships:** All authors have declared that they have no financial relationships at present or within the previous three years with any organizations that might have an interest in the submitted work. **Other relationships:** All authors have declared that there are no other relationships or activities that could appear to have influenced the submitted work.

Acknowledgements

The authors are extremely appreciative to the reviewers for their momentous remarks and positive suggestions, which are accommodating to improving the quality of the manuscript.

References

1. Krishna MV: Hall effects on the unsteady MHD flow of the Rivlin-Ericksen fluid past an infinite vertical porous plate. Waves Random Complex Media. 1-24.
2. Mohyuddin MR: Hydromagnetic unsteady Rivlin-Ericksen third-grade flow for Stokes's second problem. Chemical Engineering Communications. 2007, 194:1201-214. 10.1080/00986440701293934
3. Banerjee A, Bhattacharyya K, Mahato SK, Verma AK, Gautam AK, Chamkha AJ: Exact solutions for 2D boundary layer flow of two types of viscoelastic fluids and heat transfer on a permeable shrinking sheet with thermal radiation and variable surface temperature: Existence of multiple solutions. Waves in Random and Complex Media. 2022, 35:527-52. 10.1080/17455030.2021.2023786
4. Gull L, Mustafa M, Haq RU: A novel model for viscoelastic fluid flow and heat near a stretchable plate using variable fluid properties: A computational study. Numerical Heat Transfer, Part B: Fundamentals. 2023, 85:649-61. 10.1080/10407790.2023.2252601
5. Abel MS, Nandeppanavar MM, Malkhed MB: Hydromagnetic boundary layer flow and heat transfer in viscoelastic fluid over a continuously moving permeable stretching surface with nonuniform heat source/sink embedded in fluid-saturated porous medium. Chemical Engineering Communications. 2009, 197:633-55. 10.1080/00986440903287742
6. Hayat T, Nadeem S, Asghar S, Siddiqui AM: Effects of Hall current on unsteady flow of a second-grade fluid in a rotating system. Chemical Engineering Communications. 2005, 192:1272-284. 10.1080/009864490515810
7. Gopal CHK, Sudhakar M, Rao SM, Krishna MV: Chemical reaction on unsteady MHD convection flow of second-grade fluid over an unbounded perpendicular absorbent plate. Advances in Materials and Processing Technologies. 2023, 10:2263-285. 10.1080/2374068X.2023.2212476
8. Raghunath K, Mohana Ramana R, Ganteda C, et al.: Processing to pass unsteady MHD flow of a second-grade fluid through a porous medium in the presence of radiation absorption exhibits diffusion thermo, Hall, and ion slip effects. Advances in Materials and Processing Technologies. 2023, 10:754-71. 10.1080/2374068X.2023.2191450
9. Mahabaleshwar US, Maranna T, Pérez LM, Nayakar SNR: An effect of magnetohydrodynamic and radiation on axisymmetric flow of non-Newtonian fluid past a porous shrinking/stretching surface. Journal of Magnetism and Magnetic Materials. 2023, 571:170538. 10.1016/j.jmmm.2023.170538
10. Abbas A, Hussanan A, Ullah Z, El-Zahar ER, Seddek LF: Heat and mass transfer in magnetohydrodynamic boundary layer flow of second-grade nanofluid past inclined stretching permeable surface implanted in a porous medium. International Journal of Modelling and Simulation. 2024, 1-15. 10.1080/02286203.2024.2330993
11. Vishalakshi AB, Mahabaleshwar US, Sheikhnejad Y: Impact of MHD and mass transpiration on Rivlin-Ericksen liquid flow over a stretching sheet in a porous media with thermal communication. Transport in Porous Media. 2022, 142:353-81. 10.1007/s11242-022-01756-w
12. Javed M, Naz R: Hall and ion slip effects on the rheology of viscoelastic fluid-an application to polymers. Waves in Random and Complex Media. 2023, 35: 5453-463. 10.1080/17455030.2022.2070797
13. Kabeel AE, El-Said EM, Dafea SA: A review of magnetic field effects on flow and heat transfer in liquids: Present status and future potential for studies and applications. Renewable and Sustainable Energy Reviews. 2015, 45:830-37. 10.1016/j.rser.2015.02.029
14. Rajakumar KVB, Govinda Rao T, Umasankara Reddy M, Balamurugan KS: Influence of Dufour and thermal radiation on unsteady MHD Walter's liquid model-B flow past an impulsively started infinite vertical plate embedded in a porous medium with chemical reaction, Hall and ion slip current. SN Applied Sciences. 2020, 2:742. 10.1007/s42452-020-2484-y
15. Agunbiade SA, Dada MS: Effects of viscous dissipation on convective rotatory chemically reacting Rivlin-Ericksen flow past a porous vertical plate. Journal of Taibah University for Science. 2019, 13:402-13. 10.1080/16583655.2019.1582149
16. Gupta U, Aggarwal P, Wanchoo KR: Thermal convection of dusty compressible Rivlin-Ericksen viscoelastic fluid with Hall currents. Thermal Science. 2012, 16:177-92. 10.2298/TSCI110128113G
17. Hayat T, Khan SB, Khan M: The influence of Hall current on the rotating oscillating flows of an Oldroyd-B fluid in a porous medium. Nonlinear Dynamics. 2006, 47:353-62. 10.1007/s11071-006-9034-z
18. El-Dabe NT, Ali AR, El-Shekhipy AA, Shalaby GA: Non-linear heat and mass transfer of second grade fluid flow with Hall currents and thermophoresis effects. Applied Mathematics & Information Sciences. 2017, 11:267-80. 10.18576/amis/110133
19. Yanala DR, Kumar MA, Bejawada SG, Nisar KS, Raju RS, Rao VS: Exploration of heat and mass transfer on 3-D radiative MHD Casson fluid flow over a stretching permeable sheet with chemical reaction. Case Studies in Thermal Engineering. 2023, 51:103527. 10.1016/j.csite.2023.103527
20. Raghunath K, Mohanaramana R: Hall, Soret, and rotational effects on unsteady MHD rotating flow of a second-grade fluid through a porous medium in the presence of chemical reaction and aligned magnetic field. International Communications in Heat and Mass Transfer. 2022, 137:106287. 10.1016/j.icheatmasstransfer.2022.106287
21. Ganjikunta A, Kommaddi HB, Bhajanthri V, Kodi R: An unsteady MHD flow of a second-grade fluid passing through a porous medium in the presence of radiation absorption exhibits Hall and ion slip effects. Heat Transfer. 2023, 52:780-806. 10.1002/htj.22716
22. Jiang X, Zhang H, Wang S: Unsteady magnetohydrodynamic flow of generalized second grade fluid through porous medium with Hall effects on heat and mass transfer. Physics of Fluids. 2020, 32:113105. 10.1063/5.0032821
23. Kabeel AE, El-Said EM, Dafea SA: A review of magnetic field effects on flow and heat transfer in liquids: Present status and future potential for studies and applications. Renewable and Sustainable Energy Reviews. 2015, 45:830-37. 10.1016/j.rser.2015.02.029
24. Johnson AB, Olajuwon BI: Impact of radiation and heat generation/absorption in a Walters' B fluid through a porous medium with thermal and thermo diffusion in the presence of chemical reaction. International Journal of Modelling and Simulation. 2022, 43:87-100. 10.1080/02286203.2022.2035948
25. Nagaraju L, Naikoti K, Krishna MV: Chemical reaction and Soret effects on MHD convective flow of second-grade fluid through an absorbent medium with ramped wall temperature as well as ramped surface

concentration. Journal of the Indian Chemical Society. 2023, 100:100818. 10.1016/j.jics.2022.100818
26. Srinivasacharya D, Kaladhar K: Mixed convection flow of chemically reacting couple stress fluid in a vertical channel with Soret and Dufour effects. International Journal for Computational Methods in Engineering Science and Mechanics. 2014, 15:413-21. 10.1080/15502287.2014.915251
27. Ganesan P, Suganthi RK, Loganathan P: Soret and Dufour effects in a free convective doubly stratified flow over a vertical plate with chemical reaction. European Journal of Computational Mechanics. 2012, 200:514-31. 10.1080/00986445.2012.712580
28. Krishna Murthy SVSSNVG, Kumar V: MHD forces on double diffusive free convection process along a vertical wavy surface embedded in a doubly stratified fluid-saturated Darcy porous medium under the influence of Soret and Dufour effect. European Journal of Computational Mechanics. 2018, 27:33-57. 10.1080/17797179.2018.1439150
29. Idowu AS, Falodun BO: Soret-Dufour effects on MHD heat and mass transfer of Walter's-B viscoelastic fluid over a semi-infinite vertical plate: Spectral relaxation analysis. Journal of Taibah University for Science. 2018, 13:49-62. 10.1080/16583655.2018.1523527
30. Gbadeyan JA, Oyekunle TL, Fasogbon PF, Abubakar JU: Soret and Dufour effects on heat and mass transfer in chemically reacting MHD flow through a wavy channel. Journal of Taibah University for Science. 2018, 12:631-51. 10.1080/16583655.2018.1492221
31. Algehyne EA, Aldhabani MS, Saeed A, Dawar A, Kumam P: Mixed convective flow of Casson and Oldroyd-B fluids through a stratified stretching sheet with nonlinear thermal radiation and chemical reaction. Journal of Taibah University for Science. 2022, 16:193-203. 10.1080/16583655.2022.2040281